

Preprint no. 29/2010

An Adaptive Finite Element Approximation of a Generalised Ambrosio–Tortorelli Functional

S. Burke and C. Ortner and E. Süli

The Francfort–Marigo model of brittle fracture is posed in terms of the minimization of a highly irregular energy functional. A successful method for discretizing the model is to work with an approximation of the energy. In this work a generalised Ambrosio–Tortorelli functional is used. This leads to a bound-constrained minimization problem, which can be posed in terms of a variational inequality. We propose, analyse and implement an adaptive finite element method for computing (local) minimizers of the generalised functional.

Key words and phrases: adaptive finite element method, variational inequality, Ambrosio–Tortorelli functional, brittle fracture

The work reported here forms part of the research programme of OxMOS.

OxMOS: New Frontiers in the Mathematics of Solids
Mathematical Institute
University of Oxford
<http://www2.maths.ox.ac.uk/oxmos/>

August, 2010

AN ADAPTIVE FINITE ELEMENT APPROXIMATION OF A GENERALISED AMBROSIO–TORTORELLI FUNCTIONAL

SIOBHAN BURKE, CHRISTOPH ORTNER AND ENDRE SÜLI¹

Abstract. The Francfort–Marigo model of brittle fracture is posed in terms of the minimization of a highly irregular energy functional. A successful method for discretizing the model is to work with an approximation of the energy. In this work a generalised Ambrosio–Tortorelli functional is used. This leads to a bound-constrained minimization problem, which can be posed in terms of a variational inequality. We propose, analyse and implement an adaptive finite element method for computing (local) minimizers of the generalised functional.

1991 Mathematics Subject Classification. 65N30, 74R10, 74G65, 74G15.

August 19, 2010.

1. INTRODUCTION

The Francfort–Marigo model of quasi-static brittle fracture [26] is a new model in fracture mechanics for the prediction of crack growth in brittle materials. It is formulated in terms of a free-discontinuity problem, in which the path of the crack is itself an unknown variable. It is thus free from one of the major constraints for many models from classical fracture mechanics, that of needing a pre-defined crack path. A brief description of the model is given in Section 1.2.

In practice, the Francfort–Marigo model requires a highly irregular energy functional to be minimized, which poses difficulties for numerical approaches that are based on a direct discretization of the problem. As such, there exist a number of numerical schemes in the literature that minimize a regularisation of the energy. The Ambrosio–Tortorelli functional is one such regularisation, which can be understood as a phase-field model for the crack set. An approximation of the Francfort–Marigo model via the minimization of the *standard* Ambrosio–Tortorelli functional was proposed by Bourdin, Francfort and Marigo [10] and implemented for a range of examples by Bourdin [8, 9]. In addition, an adaptive finite element method for computing numerical solutions of this approximation was proposed and analysed by Burke, Ortner and Süli [15].

Although previous numerical schemes have focused on approximating the Francfort–Marigo energy by the standard Ambrosio–Tortorelli functional, there in fact exist an entire family of approximating generalised functionals [12, 24]. In this paper we consider the minimization of a generalised functional together with a new method for implementing crack irreversibility, which is based on a monotonicity condition specified by Giacomini [27]. This will be presented in Section 1.3. Our motivation for considering this generalisation is to investigate the possibility of selecting a functional so that the resulting minimization problem has certain desirable properties. For example, the profile of a minimizer may allow it to be resolved more easily by a numerical discretization or the minimized energy may be closer to that of the exact solution.

Keywords and phrases: adaptive finite element method, variational inequality, Ambrosio–Tortorelli functional, brittle fracture

¹ Mathematical Institute, University of Oxford, 24-29 St Giles', Oxford, OX1 3LB

The minimization of the generalised Ambrosio–Tortorelli functional can be posed in terms of a variational equality and inequality (see Section 2), the solutions of which possess an interior layer in the vicinity of the crack. It is therefore necessary to have a sufficiently fine spatial discretisation within this layer to resolve the full behaviour of the solution, however, elsewhere a coarser discretisation will suffice. Since the location of the crack is unknown a priori we propose using an adaptive finite element method to compute numerical minimizers, in which the mesh-refinement is driven by a pair of residual estimates. These are presented in Section 4.2 and an adaptive algorithm that combines mesh-refinement with an alternating minimization algorithm is given in Section 4.3. The convergence of the algorithm is analysed in Section 4.5 and we conclude by presenting some computational results in Section 6.

1.1. Notation

Throughout the paper, we assume that $m, N \in \mathbb{N}$ with $N \geq 2$. We also assume that Ω is a connected and bounded open domain in \mathbb{R}^N . For $p \in [1, \infty]$, we use $L^p(\Omega)$ to denote the standard Lebesgue spaces on Ω and $H^1(\Omega)$ to denote the standard Hilbertian Sobolev space on Ω . The N -dimensional Lebesgue and Hausdorff measures are denoted by \mathcal{L}^N and \mathcal{H}^N , respectively.

The distributional derivative of a function $f \in L^1(\Omega; \mathbb{R}^m)$ is denoted by Df . For the case $m = N$, the symmetrised distributional derivative of f is given by $\mathcal{E}(f) := \frac{1}{2}(Df + Df^T)$.

For $A, B \in \mathbb{R}^{N \times N}$ we define, using the summation convention, $A : B := A_{ij}B_{ij}$ and $|A| := (A : A)^{1/2}$. For $a \in \mathbb{R}^N$ we define the standard Euclidean norm $|a| := (a^T a)^{1/2}$. For $a, b \in \mathbb{R}^N$ we define the *tensor product* $a \otimes b$ to be the $N \times N$ matrix with entries $(a_i b_j)_{i,j=1}^N$, and the *symmetrised tensor product* $a \odot b := \frac{1}{2}(a \otimes b + b \otimes a)$.

1.2. The Francfort–Marigo Model of Brittle Fracture

We wish to introduce the model in the setting of general linearized elasticity, incorporating anti-plane strain, plane strain and three-dimensional elasticity into one unified framework. It is first necessary to define the spaces of special functions of bounded variation and special functions of bounded deformation, although we note that a knowledge of these spaces is not needed for the main part of the paper.

We say that a function $f \in L^1(\Omega; \mathbb{R})$ has bounded variation, if

$$\sup \left\{ \int_{\Omega} f \operatorname{div} \varphi \, dx : \varphi \in C_0^1(\Omega; \mathbb{R}^N), \|\varphi\|_{L^\infty(\Omega)} \leq 1 \right\} < \infty.$$

We say that a function $g \in L^1(\Omega; \mathbb{R}^N)$ has bounded deformation, if

$$\sup \left\{ \int_{\Omega} g \cdot \operatorname{div} \left(\frac{\varphi + \varphi^T}{2} \right) \, dx : \varphi \in C_0^1(\Omega; \mathbb{R}^{N \times N}), \|\varphi\|_{L^\infty(\Omega)} \leq 1 \right\} < \infty.$$

The spaces of functions of bounded variation and bounded deformation are denoted by $BV(\Omega; \mathbb{R})$ and $BD(\Omega; \mathbb{R}^N)$, respectively.

Given a function $f \in BV(\Omega; \mathbb{R})$ the distributional derivative of f can be decomposed as

$$Df = \nabla f \mathcal{L}^N + (f^+(x) - f^-(x)) \otimes \nu_f(x) \mathcal{H}^{N-1} \llcorner J(f) + D^c f,$$

where ∇f is called the *approximate gradient* of f , $J(f)$ is the *jump set* of f , ν_f is the *unit normal* to $J(f)$, f^\pm are the *inner and outer traces* of f on $J(f)$ with respect to ν_f , and $D^c f$ is called the *Cantor part* of the derivative. We refer to [3] for the precise definitions of these terms.

Given a function $g \in BD(\Omega; \mathbb{R}^N)$, the symmetrised distributional derivative of g can be decomposed as

$$\mathcal{E}(g) = e(g) \mathcal{L}^N + (g^+(x) - g^-(x)) \odot \nu_g \mathcal{H}^{N-1} \llcorner J(g) + \mathcal{E}^c g,$$

where $e(g)$ is the *approximate symmetrised gradient* of g , $J(g)$ is the *jump set* of g , ν_g is the *unit normal* to $J(g)$, g^\pm are the *inner* and *outer traces* of g on $J(g)$ with respect to ν_g , and $\mathcal{E}^c g$ is called the *Cantor part* of the derivative; see [2] for precise definitions of these terms.

The spaces of special functions of bounded variation and special functions of bounded deformation are then defined, respectively, as

$$\text{SBV}(\Omega; \mathbb{R}) := \{f \in \text{BV}(\Omega; \mathbb{R}) : D^c f = 0\} \quad \text{and} \quad \text{SBD}(\Omega; \mathbb{R}^N) := \{f \in \text{BD}(\Omega; \mathbb{R}^N) : \mathcal{E}^c(f) = 0\}.$$

We now present a brief description of the Francfort–Marigo model of brittle fracture [26]. We consider a linearly elastic body whose crack-free reference configuration is denoted by Ω . In addition to being open, bounded and connected we assume that Ω possesses a Lipschitz boundary $\partial\Omega$ (although we shall later on relax this assumption). We wish to study how the body evolves in time under the action of a varying load $g(t)$, which is applied on an open subset $\Omega_D \subset \Omega$ of positive N -dimensional Lebesgue measure. The fact that the Dirichlet condition is imposed on a set of positive N -dimensional Lebesgue measure is mostly technical and ensures that the jump set on the *Dirichlet boundary* $\partial\Omega_D \cap \Omega$ is well-defined. We call $\partial\Omega_N := \partial\Omega \setminus \partial\Omega_D$ the *Neumann boundary*.

We assume that

$$g \in L^\infty(0, T; W^{1,\infty}(\Omega; \mathbb{R}^m)) \cap W^{1,1}(0, T; H^1(\Omega; \mathbb{R}^m)),$$

so that the resulting displacement of the whole body $u : \Omega \rightarrow \mathbb{R}^m$. When $N = 2$, we assume that $m = 1$ or $m = 2$ and when $N \geq 3$, we assume that $m = N$. We refer to the anti-plane strain case as taking $N = 2$ and $m = 1$, the plane strain case as taking $N = m = 2$ and the three-dimensional elasticity case as taking $N = m = 3$.

At each time $t \in [0, T]$, we denote the set of admissible displacements of the body by $\mathcal{A}(t)$. The precise nature of $\mathcal{A}(t)$ is dependent on the value of m and will be taken as follows:

Case 1: When $m = 1$,

$$\mathcal{A}(t) := \{u \in \text{SBV}(\Omega; \mathbb{R}) : u|_{\Omega_D} = g(t)|_{\Omega_D}\}.$$

Case 2: When $m \geq 2$,

$$\mathcal{A}(t) := \{u \in \text{SBD}(\Omega; \mathbb{R}^m) : u|_{\Omega_D} = g(t)|_{\Omega_D}, \|u\|_{L^\infty(\Omega)} \leq M\},$$

for some constant $M < \infty$, which is independent of t .

The L^∞ -bound on u in the case when $m \geq 2$ is imposed for technical reasons that are related to compactness results. When $m = 1$ this bound follows from a truncation argument using the assumption that $g \in L^\infty(\Omega)$, see [27].

The Francfort–Marigo model is formulated in terms of the energy of the body, which will now be defined. For each $u \in \mathcal{A}(t)$, $t \in [0, T]$, we define the bulk energy by

$$E_B(u) := \int_{\Omega} A \nabla u : \nabla u \, dx \quad \text{for } u \in \mathcal{A}(t),$$

where $A \in \mathbb{R}^{(m \times N)^2}$ is the elasticity tensor. We assume that A possesses major symmetry for all $m, N \in \mathbb{N}$; minor symmetries when $m = N$ and that there exist positive constants C_B and C_K satisfying:

$$1. |AP| \leq C_B |P| \text{ for all } P \in \mathbb{R}^{N \times m}; \tag{1}$$

$$2. AP : P \geq 0 \text{ for all } P \in \mathbb{R}^{N \times m}; \tag{2}$$

$$3. \int_{\Omega} A \nabla u : \nabla u \, dx \geq C_K \|\nabla u\|_{L^2(\Omega)}^2 \text{ for all } u \in H^1(\Omega; \mathbb{R}^m) \text{ such that } u|_{\Omega_D} = 0. \tag{3}$$

For each Hausdorff measurable set Γ , we define the surface energy by

$$E_S(\Gamma) := \kappa \mathcal{H}^{N-1}(\Gamma),$$

where the positive constant κ is known as the *fracture toughness* of the body. This reflects Griffith's principle that, to create a crack one has to *spend* an amount of elastic energy that is proportional to the area of the crack created [28].

For each $u \in \mathcal{A}(t)$, $t \in [0, T]$ and each Hausdorff measurable set Γ , we define the total energy by

$$E(u, \Gamma) := \begin{cases} E_B(u) + E_S(\Gamma), & \text{if } \mathcal{H}^{N-1}(J(u) \setminus \Gamma) = 0, \\ +\infty, & \text{otherwise.} \end{cases}$$

The crack set Γ and the jump set $J(u)$ are decoupled in the definition of the total energy to allow for the possibility that the displacement is continuous on a subset of the crack. This decoupling also enables the irreversibility of the crack evolution to be imposed.

We introduce the Francfort–Marigo model in a time-discrete formulation. Let the time-interval $[0, T]$ be discretized as follows:

$$0 = t_0 < t_1 < \dots < t_\Lambda = T,$$

where $\Lambda \in \mathbb{N}$, $\Lambda \geq 2$. Define $\Delta t := \max \{t_k - t_{k-1} : k = 1, \dots, \Lambda\}$. Given an initial crack $\Gamma(0)$ (which, for technical reasons, should be the jump set of a function $u(0) \in \mathcal{A}(0)$); for $k = 1, \dots, \Lambda$, we seek $(u(t_k), \Gamma(t_k))$ such that the following two properties hold:

1. *Irreversibility*: $\Gamma(t_k) \supset \Gamma(t_{k-1})$;
2. *Global stability*: $E(u(t_k), \Gamma(t_k)) \leq E(\hat{u}, \hat{\Gamma}) \quad \forall \hat{u} \in \mathcal{A}(t_k) \text{ and } \forall \hat{\Gamma} \supset \Gamma(t_{k-1})$.

In practice, this formulation requires the successive solution of the global minimization problems: Find

$$u(t_k) \in \operatorname{argmin}_{v \in \mathcal{A}(t_k)} \{E_B(v) + E_S(J(v) \cup \Gamma(t_{k-1}))\}, \quad \Gamma(t_k) := J(u(t_k)) \cup \Gamma(t_{k-1}). \quad (4)$$

For further details of the model and the existence of solutions in both the time-discrete form and as $\Delta t \rightarrow 0$ we refer to [3, 20, 21, 25, 26]. Finally we note that although the model seeks to globally minimize the energy at each time step, for reasons stated in [15, Section 1.1], we will be satisfied with computing local minimizers in our numerical method.

1.3. A Generalised Ambrosio–Tortorelli Approximation

Finding solutions of the minimization problem (4) is a nontrivial task, due to the irregularity of the energy functional and the need to accurately measure the surface area of the crack. There exist a number of numerical methods in the literature that are based on minimizing an approximation of the energy functional $E(u, \Gamma)$, which is able to represent the crack set in a manner more readily tractable by numerical methods. This regularisation is achieved in the sense of Γ -convergence [13], which ensures that minimizers of the approximating functional converge to minimizers of E . A popular choice of regularisation is the standard Ambrosio–Tortorelli functional, which will be defined below. This is not, however, the only choice available and in this paper we consider a generalised approximation.

The generalised Ambrosio–Tortorelli functional $J_\varepsilon : H^1(\Omega; \mathbb{R}^m) \times H^1(\Omega; [0, 1]) \rightarrow \mathbb{R}$ is defined, for $0 < \eta \ll \varepsilon \ll 1$, as follows:

$$J_\varepsilon(u, v) := \int_\Omega (F(v) + \eta) A \nabla u : \nabla u \, dx + \kappa \int_\Omega (\varepsilon^{-1} G(v) + \varepsilon |\nabla v|^2) \, dx, \quad (5)$$

where $F \in C^3([0, 1])$ is an increasing function with $F(0) = 0$ and $F(1) = 1$, and $G \in C^3([0, 1])$ is a non-negative function such that $G(z) = 0$ if and only if $z = 1$. We refer to the case $F = v^2$ and $G = \frac{1}{4}(1-v)^2$ as the standard Ambrosio–Tortorelli functional.

Let us define

$$\begin{aligned} L_\varepsilon(\hat{u}, \hat{v}) &:= \begin{cases} J_\varepsilon(\hat{u}, \hat{v}), & \text{if } \hat{u} \in H^1(\Omega; \mathbb{R}^m), \hat{u} = g(t_k) \text{ on } \Omega_D, \hat{v} \in H^1(\Omega; [0, 1]), \\ +\infty, & \text{otherwise,} \end{cases} \\ L(\hat{u}, \hat{v}) &:= \begin{cases} E_B(\hat{u}) + C_S E_S(J(\hat{u})), & \text{if } \hat{u} \in \mathcal{A}(t_k), \hat{v} = 1 \text{ a.e. on } \Omega, \\ +\infty, & \text{otherwise,} \end{cases} \end{aligned}$$

where

$$C_S := 4 \int_0^1 \sqrt{G(s)} \, ds. \quad (6)$$

We expect that L_ε Γ -converges to L as $\varepsilon \rightarrow 0$, although we do not show the result ourselves. The result was shown by Braides [13, Theorem 4.14] for the anti-plane strain case, while, for the standard Ambrosio–Tortorelli functional, Chambolle [17] has shown the corresponding result for linear elasticity. We therefore believe that it should be possible to combine and extend these results to the generalised functional given above.

Although the Γ -convergence result has not yet been proven we will use J_ε as an approximation of the Francfort–Marigo energy functional. To construct an approximation of the time-discrete Francfort–Marigo model the minimization of J_ε must be supplemented with a criterion for enforcing the irreversibility of the crack. We choose to use a modification of the monotonicity condition $v_\varepsilon(t_k) \leq v_\varepsilon(t_{k-1})$, $k = 1, \dots, \Lambda$, specified by Giacomini [27], who showed that this guarantees crack irreversibility in the limit $\varepsilon, \Delta t \rightarrow 0$. We implement this monotonicity condition at time t_k , $k = 1, \dots, \Lambda$, but only on the following subset of Ω :

$$\text{MC}(t_{k-1}) := \{x \in \overline{\Omega} : v_\varepsilon(x, t_{k-1}) < \text{MCTOL}\},$$

where MCTOL is a user-specified value. Alternative methods for implementing crack irreversibility have been proposed [1, 4, 22, 31]; a nice survey of these methods is provided in the paper by Amora, Marigo and Maurini [4, Page 1220].

We therefore approximate the time-discrete Francfort–Marigo model as follows. At time $t = t_0$, find

$$(u_\varepsilon(t_0), v_\varepsilon(t_0)) \in \operatorname{argmin}\{J_\varepsilon(\hat{u}, \hat{v}) : \hat{u} \in H^1(\Omega; \mathbb{R}^N), \hat{u} = g(t_0) \text{ on } \Omega_D; \hat{v} \in H^1(\Omega; [0, 1])\}.$$

At subsequent times $t = t_k$, $k = 1, \dots, \Lambda$, find $(u_\varepsilon(t_k), v_\varepsilon(t_k))$ satisfying

$$\begin{aligned} (u_\varepsilon(t_k), v_\varepsilon(t_k)) &\in \operatorname{argmin}\{J_\varepsilon(\hat{u}, \hat{v}) : \hat{u} \in H^1(\Omega; \mathbb{R}^N), \hat{u} = g(t_k) \text{ on } \Omega_D; \\ &\hat{v} \in H^1(\Omega; [0, 1]), \hat{v} \leq v_\varepsilon(t_{k-1}) \text{ on } \text{MC}(t_{k-1})\}. \end{aligned} \quad (7)$$

The Ambrosio–Tortorelli approximation can be thought of as a phase-field model, in which the crack is represented as a diffused interface. At the fixed time $t = t_k$, the function $u_\varepsilon(t_k)$ is an approximation of the displacement of the body $u(t_k)$, with $u_\varepsilon(t_k) \rightarrow u(t_k)$ in $L^1(\Omega)$ as $\varepsilon, \Delta t \rightarrow 0$. The function $v_\varepsilon(t_k)$, which is constrained to take values in the interval $[0, 1]$, acts as a phase-field variable. The crack is approximated by the subset of the domain on which $v_\varepsilon(t_k)$ takes values close to zero, whilst the unfractured part of the body is represented by the subset of the domain on which $v_\varepsilon(t_k)$ takes values close to one. The transition layer between these two regimes has thickness of order ε .

A fundamental concern for any numerical approximation of the minimization problem (7) is that the spatial discretization be sufficiently fine in the vicinity of the crack to resolve the transition layers of the phase-field and displacement variables. Since the location of the crack is unknown a priori it is natural to use an

adaptively refined mesh to compute numerical minimizers. Such a method was presented for the standard Ambrosio–Tortorelli approximation by Burke, Ortner and Süli [15], in which an adaptive finite element method is proposed. In this paper we extend this method to the minimization of the generalised Ambrosio–Tortorelli functional, together with a bound-constraint on the phase-field variable for enforcing crack irreversibility.

2. CONTINUOUS MINIMIZATION PROBLEM AND CRITICAL POINTS

Let us now state the specific minimization problem under consideration. Motivated by our need to partition Ω for the purpose of defining a finite element approximation we shall assume that Ω is an open and bounded polyhedral domain in \mathbb{R}^N . By this, we simply mean that Ω possesses a finite partition into nondegenerate N -simplexes: *there exist open, disjoint, nondegenerate simplexes $T_1, \dots, T_K \subset \Omega$ such that $\mathcal{L}^N(\Omega \setminus \cup_k T_k) = 0$* (see also Section 3.1). In that case, it is clear that the usual trace and embedding theorems for Sobolev spaces hold on Ω .

Let ε and η be fixed and set $\kappa = 1$. Fix also the time $t = t_k$ and define the following function spaces:

$$\begin{aligned} H_g^1(\Omega) &:= \{u \in H^1(\Omega; \mathbb{R}^m) : u = g(t_k) \text{ on } \Omega_D\}, \quad \text{and} \\ H_D^1(\Omega) &:= \{u \in H^1(\Omega; \mathbb{R}^m) : u = 0 \text{ on } \Omega_D\}. \end{aligned}$$

We wish to incorporate the irreversibility condition into the function space setting for v . We therefore define the following convex subspace of $H^1(\Omega)$:

$$K := \{v \in H^1(\Omega; \mathbb{R}) : 0 \leq v(x) \leq \chi \text{ a.e. } x \in \Omega\},$$

for a given function $\chi \in H^1(\Omega; [0, 1])$. The function χ will be chosen so as to implement the monotonicity condition proposed for imposing irreversibility; the idea being that $\chi(x)$ is equal to $v(x, t_{k-1})$ for $x \in \text{MC}(t_{k-1})$ and then increases continuously to 1 away from $\text{MC}(t_{k-1})$. Since, in practice, we compute a finite element approximation to v at each time, we will restrict χ to lie in the finite element space X_h as soon as it is defined in Section 3.1, at which point we give a precise definition of the function χ to be taken.

To simplify the notation we now relabel the generalised Ambrosio–Tortorelli functional as $J : H_g^1(\Omega) \times K \rightarrow \mathbb{R}$ where

$$J(u, v) := \int_{\Omega} (F(v) + \eta) A \nabla u : \nabla u \, dx + \int_{\Omega} (\varepsilon^{-1} G(v) + \varepsilon |\nabla v|^2) \, dx.$$

The minimization problem can now be stated as follows. Find $(u, v) \in H_g^1(\Omega) \times K$ such that

$$(u, v) \in \operatorname{argmin}\{J(\hat{u}, \hat{v}) : \hat{u} \in H_g^1(\Omega); \hat{v} \in K\}. \quad (8)$$

Proposition 2.1. *The generalised Ambrosio–Tortorelli functional J is Gâteaux differentiable in $(H^1(\Omega))^m \times (H^1(\Omega) \cap L^\infty(\Omega))$: Given $(u, v) \in (H^1(\Omega))^m \times (H^1(\Omega) \cap L^\infty(\Omega))$, the Gâteaux derivative of J at (u, v) in the direction $(\varphi, \psi) \in (H^1(\Omega))^m \times (H^1(\Omega) \cap L^\infty(\Omega))$ is*

$$J'(u, v; \varphi, \psi) = \partial_u J(v; u, \varphi) + \partial_v J(u; v, \psi),$$

where the partial derivatives appearing on the right-hand side are defined by

$$\begin{aligned} \partial_u J(v; u, \varphi) &:= 2 \int_{\Omega} (F(v) + \eta) A \nabla u : \nabla \varphi \, dx, \quad \text{and} \\ \partial_v J(u; v, \psi) &:= \int_{\Omega} \left[F'(v) \psi A \nabla u : \nabla u + \varepsilon^{-1} G'(v) \psi + 2\varepsilon \nabla v \cdot \nabla \psi \right] \, dx. \end{aligned}$$

The proof is omitted since it is a straightforward calculation of the derivative.

A solution $(u, v) \in H_g^1(\Omega) \times K$ of the minimization problem (8) can be shown to satisfy the following variational equality and inequality [30, Theorem 3.7]:

$$\partial_u J(v; u, \varphi) = 0 \quad \forall \varphi \in H_D^1(\Omega), \quad (9)$$

$$\partial_v J(u; v, v - \psi) \leq 0 \quad \forall \psi \in K, \quad (10)$$

Definition 2.2. We say that $(u, v) \in H_g^1(\Omega) \times K$ is a critical point of J if both (9) and (10) are satisfied.

3. FINITE ELEMENT APPROXIMATION

3.1. Finite Element Discretization

Since we assumed that Ω is a polyhedral domain (see Section 2), we may discretize it as follows. Let \mathcal{T}_h be a subdivision of Ω into N -dimensional open simplices $T \in \mathcal{T}_h$, such that $\overline{\Omega} = \cup_{T \in \mathcal{T}_h} \overline{T}$ and $T_i \cap T_j = \emptyset$ for $T_i, T_j \in \mathcal{T}_h$ with $i \neq j$. The subdivision \mathcal{T}_h is chosen in such a way that the boundary of Ω_D is discretised as the union of faces of simplices from \mathcal{T}_h .

We define $h := \max_{T \in \mathcal{T}_h} \text{diam}(T)$ and each simplex $T \in \mathcal{T}_h$ is taken to be an affine transformation of the open unit simplex

$$\hat{T} := \{\hat{x} = (\hat{x}_1, \dots, \hat{x}_N) : 0 < \hat{x}_i, i = 1, \dots, N, 0 < \hat{x}_1 + \dots + \hat{x}_N < 1\}.$$

Each simplex $T \in \mathcal{T}_h$ is called an *element*. We assume that the subdivision is conforming, that is, the intersection of the closure of any two elements is either empty or is along an entire k -dimensional face, $0 \leq k \leq N - 1$. We also require that the subdivision is shape-regular, i.e.,

$$\sup_{T \in \mathcal{T}_h} \frac{h_T}{d_T} \leq \rho,$$

for some $\rho \in (0, \infty)$, where $h_T := \text{diam}(T)$ and d_T is the diameter of the largest N -dimensional ball contained in T .

Let $N_h \subset \mathbb{N}$ denote an index set for the vertices of \mathcal{T}_h . For a vertex with index $i \in N_h$, let x_i denote the position of the vertex and let ζ_i be the continuous piecewise linear basis function such that $\zeta_i(x_j) = \delta_{ij}$. Define $N_h^D := \{i \in N_h : x_i \in \overline{\Omega_D}\}$.

Let \mathcal{E}_h denote the set of $(N - 1)$ -dimensional open faces in the subdivision with

$$\mathcal{E}_h^D := \{e \in \mathcal{E}_h : e \subseteq \overline{\Omega_D}\}, \quad \mathcal{E}_h^N := \{e \in \mathcal{E}_h : e \subseteq \partial\Omega_N\} \quad \text{and} \quad \mathcal{E}_h^I := \{e \in \mathcal{E}_h \setminus (\mathcal{E}_h^D \cup \mathcal{E}_h^N)\}.$$

We define E_h, E_h^D, E_h^N and E_h^I as the union of all faces in $\mathcal{E}_h, \mathcal{E}_h^D, \mathcal{E}_h^N$ and \mathcal{E}_h^I , respectively. For a face $e \in E_h$ define $h_e := \text{diam}(e)$.

For all $i \in N_h$, let ω_i be the closure of the union of elements $T \in \mathcal{T}_h$ that have x_i as the position of a vertex, that is, $\omega_i := \text{supp}(\zeta_i)$. For a face $e \in \mathcal{E}_h$ and an element $T \in \mathcal{T}_h$ define

$$\omega_e := \bigcup_{i \in N_h : x_i \in \overline{e}} \omega_i \quad \text{and} \quad \omega_T := \bigcup_{i \in N_h : x_i \in \overline{T}} \omega_i.$$

We now define the piecewise linear finite element space

$$X_h := \left\{ \sum_{i \in N_h} \lambda_i \zeta_i : \lambda_i \in \mathbb{R} \right\}.$$

For simplicity we assume that the applied displacement $g \in (X_h)^m$ and define the following finite element spaces:

$$X_h^g := (X_h)^m \cap H_g^1(\Omega) \quad \text{and} \quad X_h^D := (X_h)^m \cap H_D^1(\Omega).$$

We also assume that $\chi \in X_h$ and define the finite element space

$$K_h := X_h \cap K.$$

In practice, at time $t = t_k$, we take $\chi = \sum_{i \in N_h} \chi_i \zeta_i(x)$, where

$$\chi_i := \begin{cases} 1, & \text{if } v_h(x_i, t_{k-1}) > \text{MCTOL}, \\ v_h(x_i, t_{k-1}), & \text{if } v_h(x_i, t_{k-1}) \leq \text{MCTOL}. \end{cases}$$

In the finite element approximation we wish to find $(u_h, v_h) \in X_h^g \times K_h$ such that

$$(u_h, v_h) \in \operatorname{argmin} \{J(\hat{u}_h, \hat{v}_h) : \hat{u}_h \in X_h^g, \hat{v}_h \in K_h\}. \quad (11)$$

Remark 3.1. In practice, for general functions F and G and a given $(u_h, v_h) \in X_h^g \times K_h$ it may be difficult to evaluate $J(u_h, v_h)$ exactly. As such it may be necessary to use a numerical quadrature scheme to compute the integral. However, since this is not the main focus of our work and since the algorithm will only be implemented in cases where exact integration is possible, we choose not to consider the effect of quadrature here. We will, however, briefly discuss how the results might be extended to include such a scheme in Remark 4.10.

3.2. Discrete Variational Inequality

Similarly to the continuous problem, it can be shown that a solution, $(u_h, v_h) \in X_h^g \times K_h$, of the discrete minimization problem (11) satisfies the following variational equality and inequality:

$$\partial_u J(v_h; u_h, \varphi_h) = 0 \quad \forall \varphi_h \in X_h^D, \quad (12)$$

$$\partial_v J(u_h; v_h, v_h - \psi_h) \leq 0 \quad \forall \psi_h \in K_h. \quad (13)$$

Definition 3.2. We say that $(u_h, v_h) \in X_h^g \times K_h$ is a discrete critical point of J if it satisfies both (12) and (13).

We conclude this section with a proposition showing that the variational inequality (13) becomes an equality on a subset of the domain in which the bound constraints are inactive. Before stating the proposition we first define the discrete *contact* and *non-contact* sets.

For all $v_h \in K_h$ we define the discrete contact set

$$\mathcal{C}_h(v_h) := \bigcup_{i \in N_h^c} \omega_i, \quad \text{where} \quad N_h^c := \{i \in N_h : v_h(x_i) = 0 \text{ or } v_h(x_i) = \chi(x_i)\}.$$

The discrete non-contact set is $\mathcal{N}_h(v_h) := \Omega \setminus \mathcal{C}_h(v_h)$.

Following the work of Chen and Nochetto [18], we also introduce the discrete function $\sigma_h = \sigma_h(u_h, v_h) \in X_h$, which is defined through the relation

$$\int_{\Omega} P_h(\sigma_h w_h) \, dx = \partial_v J(u_h; v_h, w_h) \quad \forall w_h \in X_h, \quad (14)$$

where $P_h : C(\overline{\Omega}) \rightarrow X_h$ is the standard nodal interpolation operator [14, Section 3.3]. For each fixed $(u_h, v_h) \in X_h^g \times K_h$, the existence and uniqueness of the function $\sigma_h(u_h, v_h) \in X_h$ follows from the Riesz Representation

Theorem [23, Appendix D]. For simplicity, we henceforth write σ_h instead of $\sigma_h(u_h, v_h)$ whenever $(u_h, v_h) \in X_h^g \times K_h$ is fixed.

Remark 3.3. Given $(u_h, v_h) \in X_h^g \times K_h$ we can evaluate $\sigma_h(x_i)$ for all $i \in N_h$ as follows:

$$\partial_v J(u_h; v_h, \zeta_i) = \int_{\Omega} P_h(\sigma_h \zeta_i) dx = \sigma_h(x_i) \int_{\omega_i} \zeta_i dx.$$

Hence,

$$\sigma_h(x_i) = \frac{1}{(1, \zeta_i)} \partial_v J(u_h; v_h, \zeta_i) \quad \forall i \in N_h,$$

where (\cdot, \cdot) denotes the standard L^2 inner product on Ω .

Proposition 3.4. Let $(u_h, v_h) \in X_h^g \times K_h$ satisfy

$$\partial_v J(u_h; v_h, v_h - \psi_h) \leq 0 \quad \forall \psi_h \in K_h. \quad (15)$$

Then, $\sigma_h(x) \equiv 0$ for all $x \in \overline{N_h}$.

Proof. Suppose that $(u_h, v_h) \in X_h^g \times K_h$ satisfies (15). Let $i \in N_h$ be such that $0 < v_h(x_i) < \chi(x_i)$. For sufficiently small $t > 0$ we have $v_h - t\zeta_i \in K_h$. Taking $\psi_h = v_h - t\zeta_i$ in (15) and dividing by t ,

$$\partial_v J(u_h; v_h, \zeta_i) \leq 0.$$

Similarly, taking $\psi_h = v_h + t\zeta_i \in K_h$ in (15) with sufficiently small $t > 0$, we have

$$\partial_v J(u_h; v_h, \zeta_i) \geq 0.$$

This implies, using Remark 3.3, that

$$\sigma_h(x_i) = \frac{1}{(1, \zeta_i)} \partial_v J(u_h; v_h, \zeta_i) = 0.$$

It thus follows that $\sigma_h(x_i) = 0$ for all $i \in N_h$ such that $0 < v_h(x_i) < \chi(x_i)$. Therefore, $\sigma_h(x) \equiv 0$ for all $x \in \overline{N_h}$. \square

3.3. Alternating Minimization Algorithm

We now describe a specific algorithm for computing numerical minimizers of J . It was originally proposed by Bourdin, Francfort and Marigo [10] for the minimization of the standard Ambrosio–Tortorelli functional. The algorithm involves minimizing the functional with respect to one variable at a time. For a user-specified termination tolerance **VTOL** the algorithm is presented below.

Alternating Minimization Algorithm

1. Input initial crack field v_h^1 .
2. For $n = 1, 2, \dots$
 - (a) $u_h^n = \operatorname{argmin} \{J(z_h, v_h^n) : z_h \in X_h^g\}$;
 - (b) $v_h^{n+1} \in \operatorname{argmin} \{J(u_h^n, z_h) : z_h \in K_h\}$;
 - (c) Repeat until $\|v_h^{n+1} - v_h^n\|_{L^\infty(\Omega)} < \text{VTOL}$.
3. Set $u_h(t_k) = u_h^n$ and $v_h(t_k) = v_h^{n+1}$.

The minimization with respect to v_h takes the form of a bound-constrained minimization problem, which may not possess a unique solution. It is therefore necessary to state a specific minimization algorithm for J with respect to v_h in order for the above algorithm to be well-defined. One such minimization algorithm will be given in Section 5. For the present, however, we assume that a minimizer of J can be computed on a fixed mesh.

4. ADAPTIVE FINITE ELEMENT APPROXIMATION

Since both the phase-field variable and the displacement variable possess an interior layer in the vicinity of the crack, it is necessary to have a sufficiently fine mesh in this region to resolve the minimizer. However, outside this layer a coarser mesh will suffice. Since we do not know the location of the crack path in advance, it is therefore a natural idea to use an adaptively refined mesh. Following established adaptive finite element theory we use a residual based *local refinement indicator* to identify those elements where mesh refinement would be most beneficial for improving the accuracy of the solution.

For a discrete critical point $(u_h, v_h) \in X_h^g \times K_h$ of J we use a posteriori upper bounds of the residuals

$$\sup_{\varphi \in H_D^1(\Omega)} \frac{|\partial_u J(v_h; u_h, \varphi)|}{\|\varphi\|_{H^1(\Omega)}} \quad (16)$$

and

$$\sup_{\psi \in K} \frac{\partial_v J(v_h; u_h, v_h - \psi)}{\|\psi\|_{H^1(\Omega)} + 1} \quad (17)$$

as refinement indicator functions for the u and v minimization problems, respectively.

4.1. Quasi-interpolation Operator

The following interpolation results will be needed for the subsequent residual estimate. Henceforth we use \lesssim to denote $\leq C$ where the positive constant C depends only on the shape-regularity parameter ρ of the mesh but not on the mesh size.

We use the quasi-interpolation operator defined by Carstensen [16]. Its definition requires us to first identify the set of *free* nodes, that is, the set of nodes on which a Dirichlet condition is not enforced. Since, in the estimate of (16) the quasi-interpolation operator will act on functions from $H_D^1(\Omega)$ on which a homogeneous Dirichlet condition is imposed, whilst, in the estimate of (17) the quasi-interpolation operator will act on functions from K on which no Dirichlet condition is enforced, we will define two quasi-interpolation operators:

$$\mathcal{I}_h^D : H_D^1(\Omega) \rightarrow X_h^D \quad \text{and} \quad \mathcal{I}_h : H^1(\Omega) \rightarrow X_h.$$

We first define \mathcal{I}_h^D ; let $N_h^F := N_h \setminus N_h^D$ and define a partition of unity, $\{\bar{\zeta}_i : i \in N_h^F\}$, as follows:

$$\bar{\zeta}_i(x) := \frac{\zeta_i(x)}{\zeta(x)} \quad \forall i \in N_h^F, \quad \text{where} \quad \zeta(x) := \sum_{i \in N_h^F} \zeta_i(x).$$

For $\varphi \in H_D^1(\Omega)$, the quasi-interpolant $\mathcal{I}_h^D \varphi \in X_h^D$ is defined as follows:

$$\mathcal{I}_h^D \varphi(x) := \sum_{i \in N_h^F} \varphi_i \zeta_i(x), \quad \text{where} \quad \varphi_i := \frac{\int_{\omega_i} \varphi \bar{\zeta}_i \, dx}{\int_{\omega_i} \bar{\zeta}_i \, dx}. \quad (18)$$

For $\psi \in H^1(\Omega)$, the quasi-interpolant $\mathcal{I}_h \psi \in X_h$ is defined as follows:

$$\mathcal{I}_h \psi(x) := \sum_{i \in N_h} \psi_i \zeta_i(x), \quad \text{where} \quad \psi_i := \frac{\int_{\omega_i} \psi \zeta_i \, dx}{\int_{\omega_i} \zeta_i \, dx}. \quad (19)$$

Note, however, that \mathcal{I}_h^D reduces to \mathcal{I}_h on taking $N_h^D = \emptyset$, so that $N_h^F = N_h$; hence, all the approximation results for \mathcal{I}_h will follow from those for \mathcal{I}_h^D .

Remark 4.1. The quasi-interpolation operators $\mathcal{I}_h^D : H_D^1(\Omega) \rightarrow X_h^D$ and $\mathcal{I}_h : H^1(\Omega) \rightarrow X_h$ are positivity preserving; that is, for all $\varphi \in H_D^1(\Omega)$ and $\psi \in H^1(\Omega)$ such that $\varphi, \psi \geq 0$ we have $\mathcal{I}_h^D \varphi \geq 0$ and $\mathcal{I}_h \psi \geq 0$.

The following local averaging property is satisfied by the quasi-interpolation operators. Let $\varphi \in H_D^1(\Omega)$ and $\psi \in H^1(\Omega)$, then

$$\int_{\omega_i} (\varphi - \varphi_i \zeta) \bar{\zeta}_i \, dx = 0 \quad \forall i \in N_h^F, \quad (20)$$

$$\int_{\omega_i} (\psi - \psi_i) \zeta_i \, dx = 0 \quad \forall i \in N_h. \quad (21)$$

We now state several approximation and stability properties satisfied by the quasi-interpolants, which are modifications of the results presented in [16].

Proposition 4.2.

(a) *There exists a constant $\hat{C}_1 > 0$, independent of ω_i , and a patch of elements $\bar{\omega}_i \supseteq \omega_i$, such that,*

$$\|(\varphi - \varphi_i \zeta) \bar{\zeta}_i\|_{L^2(\omega_i)} \leq \hat{C}_1 h_i \|\nabla \varphi\|_{L^2(\bar{\omega}_i)}, \quad \forall \varphi \in H_D^1(\Omega) \text{ and } \forall i \in N_h^F. \quad (22)$$

(b) *There exists a constant $\hat{C}_2 > 0$, independent of e , such that*

$$\|\varphi - \mathcal{I}_h^D \varphi\|_{L^2(e)} \leq \hat{C}_2 h_e^{1/2} \|\nabla \varphi\|_{L^2(\bar{\omega}_e)} \quad \forall \varphi \in H_D^1(\Omega) \text{ and } \forall e \in E_h, \quad (23)$$

where $\bar{\omega}_e := \bigcup_{i: x_i \in \bar{e}} \bar{\omega}_i$.

(c) *There exist constants $\hat{C}_3 > 0$ and $\hat{C}_4 > 0$, independent of T , such that*

$$\|\mathcal{I}_h^D \varphi\|_{L^2(T)} \leq \hat{C}_3 \|\varphi\|_{L^2(\omega_T)} \quad \text{and} \quad \|\nabla(\mathcal{I}_h^D \varphi)\|_{L^2(T)} \leq \hat{C}_4 \|\nabla \varphi\|_{L^2(\bar{\omega}_T)}, \quad (24)$$

for all $\varphi \in H_D^1(\Omega)$ and all $T \in \mathcal{T}_h$, where $\omega_T := \bigcup_{i: x_i \in T} \omega_i$ and $\bar{\omega}_T := \bigcup_{i: x_i \in T} \bar{\omega}_i$.

Properties (a) to (c) also hold on replacing \mathcal{I}_h^D with \mathcal{I}_h and $H_D^1(\Omega)$ with $H^1(\Omega)$.

The proof of Proposition 4.2 is postponed to Appendix A.

Remark 4.3. The local averaging property allows us to achieve tighter upper bounds in the estimate of the residuals. For all $f \in L^2(\Omega)$ and $\varphi \in H_D^1(\Omega)$, we have

$$\int_{\Omega} f(\varphi - \mathcal{I}_h^D \varphi) \, dx = \sum_{i \in N_h^F} \int_{\omega_i} f(\varphi - \varphi_i \zeta) \bar{\zeta}_i \, dx.$$

Therefore, using (20), we may subtract any scalars $\alpha_i \in \mathbb{R}$, $i \in N_h^F$, from f as follows:

$$\int_{\Omega} f(\varphi - \mathcal{I}_h^D \varphi) \, dx = \sum_{i \in N_h^F} \int_{\omega_i} (f - \alpha_i)(\varphi - \varphi_i \zeta) \bar{\zeta}_i \, dx.$$

Hence, using the approximation property (22),

$$\begin{aligned}
\int_{\Omega} f(\varphi - \mathcal{I}_h^D \varphi) \, dx &\leq \sum_{i \in N_h^F} \|f - \alpha_i\|_{L^2(\omega_i)} \|(\varphi - \varphi_i \zeta_i) \bar{\zeta}_i\|_{L^2(\omega_i)} \\
&\leq \sum_{i \in N_h^F} \hat{C}_1 h_i \|f - \alpha_i\|_{L^2(\omega_i)} \|\nabla \varphi\|_{L^2(\omega_i)} \\
&\lesssim \left[\sum_{i \in N_h^F} h_i^2 \|f - \alpha_i\|_{L^2(\omega_i)}^2 \right]^{1/2} \|\nabla \varphi\|_{L^2(\Omega)}.
\end{aligned}$$

It can be similarly shown that for all $f \in L^2(\Omega)$ and $\psi \in H^1(\Omega)$ we have

$$\int_{\Omega} f(\psi - \mathcal{I}_h \psi) \, dx \lesssim \left[\sum_{i \in N_h} h_i^2 \|f - \alpha_i\|_{L^2(\omega_i)}^2 \right]^{1/2} \|\nabla \psi\|_{L^2(\Omega)}.$$

In the residual estimates, we will take α_i to be the following average of f in ω_i , for each $i \in N_h^F$:

$$\alpha_i := \bar{f}_i := \frac{1}{|\omega_i|} \int_{\omega_i} f \, dx. \quad (25)$$

4.2. Residual Estimate

Before stating the main proposition of this section it will be useful to adopt the following definitions. For all $u_h \in X_h^g$ and $e \in \mathcal{E}_h$, with unit normal vector n , we define

$$\llbracket A \nabla u_h \rrbracket_e := \begin{cases} |(A \nabla u_h|_{T_1} - A \nabla u_h|_{T_2}) n|, & \text{if } e \subseteq E_h \setminus \partial\Omega, \text{ with } e = \bar{T}_1 \cap \bar{T}_2 \\ & \text{for some } T_1, T_2 \in \mathcal{T}_h, \\ |(A \nabla u_h) n|_e, & \text{if } e \subseteq \partial\Omega. \end{cases}$$

For all $v_h \in K_h$ and $e \in \mathcal{E}_h$ we define

$$\llbracket \nabla v_h \rrbracket_e := \begin{cases} |\nabla v_h|_{T_1} - \nabla v_h|_{T_2}|, & \text{if } e \subseteq E_h \setminus \partial\Omega, \text{ with } e = \bar{T}_1 \cap \bar{T}_2 \text{ for some } T_1, T_2 \in \mathcal{T}_h, \\ |\nabla v_h \cdot n|_e, & \text{if } e \subseteq \partial\Omega, \end{cases}$$

where n is the outer unit normal to $\partial\Omega$.

Proposition 4.4. *Let $(u_h, v_h) \in X_h^g \times K_h$ be such that*

$$\partial_u J(v_h; u_h, \varphi_h) = 0 \quad \forall \varphi_h \in X_h^D, \quad (26)$$

$$\partial_v J(u_h; v_h, v_h - \psi_h) \leq 0 \quad \forall \psi_h \in K_h. \quad (27)$$

Then,

$$\begin{aligned}
|\partial_u J(v_h; u_h, \varphi)| &\lesssim \mu_h \|\nabla \varphi\|_{L^2(\Omega)} \quad \forall \varphi \in H_D^1(\Omega), \\
\partial_v J(u_h; v_h; v_h - \psi) &\lesssim \nu_h (\|\psi\|_{H^1(\Omega)} + 1) \quad \forall \psi \in K,
\end{aligned}$$

where μ_h and ν_h are defined as follows:

$$\mu_h(u_h, v_h) := \left[\sum_{T \in \mathcal{T}_h} |\mu_T(u_h, v_h)|^2 \right]^{1/2}, \quad \nu_h(u_h, v_h) := \left[\sum_{T \in \mathcal{T}_h} |\nu_T(u_h, v_h)|^2 \right]^{1/2},$$

where,

$$|\mu_T(u_h, v_h)|^2 := \sum_{\substack{i \in N_h^F: \\ x_i \in \bar{T}}} h_i^2 \|p - \bar{p}_i\|_{L^2(\omega_i)}^2 + 4 \sum_{e \subseteq \partial T \setminus E_h^D} h_e \| (F(v_h) + \eta) \llbracket A \nabla u_h \rrbracket_e \|_{L^2(e)}^2,$$

$$p(u_h, v_h) := 2F'(v_h)(A \nabla u_h) \nabla v_h,$$

$$|\nu_T(u_h, v_h)|^2 := \begin{cases} |\nu_T^1(u_h, v_h)|^2 + |\nu_T^2(u_h, v_h)|^2, & \text{if } T \subseteq \mathcal{C}_h(v_h), \\ |\nu_T^1(u_h, v_h)|^2, & \text{if } T \subseteq \mathcal{N}_h(v_h), \end{cases}$$

$$|\nu_T^1(u_h, v_h)|^2 := \sum_{i: x_i \in \bar{T}} h_i^2 \|q - \bar{q}_i\|_{L^2(\omega_i)}^2 + 4\varepsilon^2 \sum_{e \subseteq \partial T} h_e \|\llbracket \nabla v_h \rrbracket_e\|_{L^2(e)}^2,$$

$$|\nu_T^2(u_h, v_h)|^2 := \sum_{i: x_i \in \bar{T}} \left[h_T^{N/2} \|q\|_{L^2(T)} + \varepsilon \sum_{\substack{e \subseteq \partial T \setminus \partial \mathcal{C}_h(v_h): \\ x_i \in \bar{e}}} h_e^{N-1} \llbracket \nabla v_h \rrbracket_e \right] \text{osc}_h(\chi; \omega_i),$$

$$q(u_h, v_h) := F'(v_h) A \nabla u_h : \nabla u_h + \varepsilon^{-1} G'(v_h),$$

$$\text{osc}_h(\chi; \omega_i) := \frac{1}{|(1, \zeta_i)|} \left| \sum_{j: x_j \in \bar{\omega}_i} (\chi(x_i) - \chi(x_j)) \int_{\omega_i} \zeta_j \zeta_i \, dx \right|.$$

Proof.

Part 1. Let us fix $\varphi \in H_D^1(\Omega)$ and consider first the functional $\varphi \mapsto \partial_u J(v_h; u_h, \varphi)$. The bound for this term is a standard residual estimate with the quasi-interpolant defined in (18).

Since (u_h, v_h) satisfies (26),

$$\partial_u J(v_h; u_h, \varphi) = \partial_u J(v_h; u_h, \varphi - \varphi_h),$$

for all $\varphi_h \in X_h^D$. Hence,

$$\begin{aligned} \partial_u J(v_h; u_h, \varphi) &= \sum_{T \in \mathcal{T}_h} 2 \int_T (F(v_h) + \eta) A \nabla u_h : \nabla (\varphi - \varphi_h) \, dx \\ &= \sum_{T \in \mathcal{T}_h} \left[-2 \int_T \text{div}((F(v_h) + \eta) A \nabla u_h) \cdot (\varphi - \varphi_h) \, dx \right. \\ &\quad \left. + 2 \int_{\partial T} ((F(v_h) + \eta) (A \nabla u_h) n) \cdot (\varphi - \varphi_h) \, ds \right] \\ &= -2 \int_{\Omega} (F'(v_h) (A \nabla u_h) \nabla v_h) \cdot (\varphi - \varphi_h) \, dx \\ &\quad + \sum_{T \in \mathcal{T}_h} 2 \int_{\partial T} ((F(v_h) + \eta) (A \nabla u_h) n) \cdot (\varphi - \varphi_h) \, ds. \end{aligned}$$

To simplify the expression let us define

$$p(u_h, v_h) := 2F'(v_h)(A \nabla u_h) \nabla v_h.$$

We, therefore, have

$$|\partial_u J(v_h; u_h, \varphi)| \leq \left| \int_{\Omega} p \cdot (\varphi - \varphi_h) dx \right| + \left| \sum_{T \in \mathcal{T}_h} 2 \int_{\partial T} ((F(v_h) + \eta)(A \nabla u_h) n) \cdot (\varphi - \varphi_h) ds \right|,$$

for all $\varphi_h \in X_h^D$. We choose $\varphi_h = \mathcal{I}_h^D \varphi$; hence, using Remark 4.3,

$$\left| \int_{\Omega} p \cdot (\varphi - \varphi_h) dx \right| \lesssim \left[\sum_{i \in N_h^F} h_i^2 \|p - \bar{p}_i\|_{L^2(\omega_i)}^2 \right]^{1/2} \|\nabla \varphi\|_{L^2(\Omega)},$$

where \bar{p}_i is defined in (25).

We estimate the edge terms using approximation property (23) as follows

$$\begin{aligned} & \left| \sum_{T \in \mathcal{T}_h} 2 \int_{\partial T} ((F(v_h) + \eta)(A \nabla u_h) n) \cdot (\varphi - \varphi_h) ds \right| \\ & \lesssim \sum_{e \subseteq E_h \setminus E_h^D} 2 \| (F(v_h) + \eta) \llbracket A \nabla u_h \rrbracket_e \|_{L^2(e)} \|\varphi - \varphi_h\|_{L^2(e)} \\ & \lesssim \sum_{e \subseteq E_h \setminus E_h^D} 2 \| (F(v_h) + \eta) \llbracket A \nabla u_h \rrbracket_e \|_{L^2(e)} h_e^{1/2} \|\nabla \varphi\|_{L^2(\bar{\omega}_e)} \\ & \lesssim \left[\sum_{e \subseteq E_h \setminus E_h^D} 4 h_e \| (F(v_h) + \eta) \llbracket A \nabla u_h \rrbracket_e \|_{L^2(e)}^2 \right]^{1/2} \|\nabla \varphi\|_{L^2(\Omega)}. \end{aligned}$$

Hence,

$$\begin{aligned} |\partial_u J(v_h; u_h, \varphi)| & \lesssim \left[\sum_{i \in N_h^F} h_i^2 \|p - \bar{p}_i\|_{L^2(\omega_i)}^2 \right. \\ & \quad \left. + 4 \sum_{e \subseteq E_h \setminus E_h^D} h_e \| (F(v_h) + \eta) \llbracket A \nabla u_h \rrbracket_e \|_{L^2(e)}^2 \right]^{1/2} \|\nabla \varphi\|_{L^2(\Omega)} \\ & \lesssim \left[\sum_{T \in \mathcal{T}_h} \left(\sum_{\substack{i \in N_h^F \\ x_i \in \bar{T}}} h_i^2 \|p - \bar{p}_i\|_{L^2(\omega_i)}^2 \right. \right. \\ & \quad \left. \left. + 4 \sum_{e \subseteq \partial T \setminus E_h^D} h_e \| (F(v_h) + \eta) \llbracket A \nabla u_h \rrbracket_e \|_{L^2(e)}^2 \right) \right]^{1/2} \|\nabla \varphi\|_{L^2(\Omega)}. \end{aligned}$$

Therefore,

$$|\partial_u J(v_h; u_h, \varphi)| \lesssim \left[\sum_{T \in \mathcal{T}_h} |\mu_T(u_h, v_h)|^2 \right]^{1/2} \|\nabla \varphi\|_{L^2(\Omega)},$$

where

$$|\mu_T(u_h, v_h)|^2 := \sum_{\substack{i \in N_h^F: \\ x_i \in \bar{T}}} h_i^2 \|p - \bar{p}_i\|_{L^2(\omega_i)}^2 + 4 \sum_{e \subseteq \partial T \setminus E_h^D} h_e \| (F(v_h) + \eta) \llbracket A \nabla u_h \rrbracket_e \|_{L^2(e)}^2.$$

Part 2 Fix $\psi \in K$ and consider the functional $\psi \rightarrow \partial_v J(u_h; v_h, v_h - \psi)$.

Since we have assumed that (u_h, v_h) satisfies (27),

$$\begin{aligned} \partial_v J(u_h; v_h, v_h - \psi) &\leq \partial_v J(u_h; v_h, v_h - \psi) + \partial_v J(u_h; v_h, \psi_h - v_h) \\ &= -\partial_v J(u_h; v_h, \psi) + \partial_v J(u_h; v_h, \psi_h), \end{aligned}$$

for all $\psi_h \in K_h$. Hence,

$$\begin{aligned} |\partial_v J(u_h; v_h, v_h - \psi)| &\leq |\partial_v J(u_h; v_h, \mathcal{I}_h \psi - \psi)| \\ &\quad + |\partial_v J(u_h; v_h, \psi_h - \mathcal{I}_h \psi)|, \end{aligned} \tag{28}$$

where $\mathcal{I}_h \psi$ is the quasi-interpolant defined in (19). We estimate the first and second terms from (28) in Part 2(a) and Part 2(b), respectively. The first term will be bounded in a similar way to Part 1, whilst the second term will be bounded in terms of the obstacle χ .

Part 2(a) For ease of notation we define

$$q(u_h, v_h) := F'(v_h) A \nabla u_h : \nabla u_h + \varepsilon^{-1} G'(v_h),$$

then

$$\begin{aligned} \partial_v J(u_h; v_h, \mathcal{I}_h \psi - \psi) &= \int_{\Omega} q(\mathcal{I}_h \psi - \psi) \, dx + 2\varepsilon \int_{\Omega} \nabla v_h \cdot \nabla (\mathcal{I}_h \psi - \psi) \, dx \\ &= \int_{\Omega} q(\mathcal{I}_h \psi - \psi) \, dx + 2\varepsilon \sum_{T \in \mathcal{T}_h} \int_{\partial T} \nabla v_h \cdot n (\mathcal{I}_h \psi - \psi) \, ds. \end{aligned} \tag{29}$$

We estimate the first term in (29) in an identical manner to Part 1 to obtain

$$\left| \int_{\Omega} q(\mathcal{I}_h \psi - \psi) \, dx \right| \lesssim \left[\sum_{i \in N_h} h_i^2 \|q - \bar{q}_i\|_{L^2(\omega_i)}^2 \right]^{1/2} \|\nabla \psi\|_{L^2(\Omega)}.$$

The second term in (29) is estimated using the approximation property (23) as follows:

$$\begin{aligned} \left| \sum_{T \in \mathcal{T}_h} \int_{\partial T} \nabla v_h \cdot n (\mathcal{I}_h \psi - \psi) \, ds \right| &\lesssim \sum_{e \subseteq E} \|[\nabla v_h]_e\|_{L^2(e)} \|\mathcal{I}_h \psi - \psi\|_{L^2(e)} \\ &\lesssim \sum_{e \subseteq E} \|[\nabla v_h]_e\|_{L^2(e)} h_e^{1/2} \|\nabla \psi\|_{L^2(\bar{\omega}_e)} \\ &\lesssim \left[\sum_{e \subseteq E} h_e \|[\nabla v_h]_e\|_{L^2(e)}^2 \right]^{1/2} \|\nabla \psi\|_{L^2(\Omega)}. \end{aligned}$$

Hence

$$\begin{aligned}
& |\partial_v J(u_h; v_h, \mathcal{I}_h \psi - \psi)| \\
& \lesssim \left[\sum_{i \in N_h} h_i^2 \|q - \bar{q}_i\|_{L^2(\omega_i)}^2 + 4\varepsilon^2 \sum_{e \subseteq E} h_e \|\llbracket \nabla v_h \rrbracket_e\|_{L^2(e)}^2 \right]^{1/2} \|\nabla \psi\|_{L^2(\Omega)} \\
& \lesssim \left[\sum_{T \in \mathcal{T}_h} \left(\sum_{i: x_i \in \bar{T}} h_i^2 \|q - \bar{q}_i\|_{L^2(\omega_i)}^2 + 4\varepsilon^2 \sum_{e \subseteq \partial T} h_e \|\llbracket \nabla v_h \rrbracket_e\|_{L^2(e)}^2 \right) \right]^{1/2} \|\nabla \psi\|_{L^2(\Omega)} \\
& = \left[\sum_{T \in \mathcal{T}_h} |\nu_T^1(u_h, v_h)|^2 \right]^{1/2} \|\nabla \psi\|_{L^2(\Omega)}.
\end{aligned}$$

Part 2(b) We now consider the second term in (28). For all $\psi_h \in K_h$, it follows from (14) and Proposition 3.4 that

$$\begin{aligned}
|\partial_v J(u_h; v_h, \psi_h - \mathcal{I}_h \psi)| &= \left| \int_{\Omega} P_h(\sigma_h(\psi_h - \mathcal{I}_h \psi)) \, dx \right| \\
&= \left| \sum_{i \in N_h} \sigma_h(x_i)(\psi_h(x_i) - \mathcal{I}_h \psi(x_i)) \int_{\omega_i} \zeta_i \, dx \right| \\
&= \left| \sum_{i \in N_h^c} \sigma_h(x_i)(\psi_h(x_i) - \mathcal{I}_h \psi(x_i)) \int_{\omega_i} \zeta_i \, dx \right|.
\end{aligned}$$

Thus, using Remark 3.3,

$$|\partial_v J(u_h; v_h, \psi_h - \mathcal{I}_h \psi)| \leq \sum_{i \in N_h^c} |\partial_v J(u_h; v_h, \zeta_i)| |\psi_h(x_i) - \mathcal{I}_h \psi(x_i)|.$$

The term $|\partial_v J(u_h; v_h, \zeta_i)|$ is estimated as follows:

$$\begin{aligned}
|\partial_v J(u_h; v_h, \zeta_i)| &= \left| \int_{\omega_i} (q\zeta_i + \varepsilon \nabla v_h \cdot \nabla \zeta_i) \, dx \right| \\
&\leq \sum_{T \subseteq \omega_i} \int_T |q| \zeta_i \, dx + \varepsilon \left| \sum_{T \subseteq \omega_i} \int_{\partial T} \nabla v_h \cdot n \zeta_i \, dx \right| \\
&\leq \sum_{T \subseteq \omega_i} h_T^{N/2} \|q\|_{L^2(T)} + \varepsilon \sum_{e \subset \omega_i \setminus \partial \omega_i} h_e^{N-1} \|\llbracket \nabla v_h \rrbracket_e\|.
\end{aligned}$$

Therefore,

$$\begin{aligned}
& |\partial_v J(u_h; v_h, \psi_h - \mathcal{I}_h \psi)| \\
& \leq \sum_{i \in N_h^c} \left[\sum_{T \subseteq \omega_i} h_T^{N/2} \|q\|_{L^2(T)} + \varepsilon \sum_{e \subset \omega_i \setminus \partial \omega_i} h_e^{N-1} \|\llbracket \nabla v_h \rrbracket_e\| \right] |\psi_h(x_i) - \mathcal{I}_h \psi(x_i)|.
\end{aligned}$$

Clearly, we would like to choose $\psi_h = \mathcal{I}_h \psi$; however, $\mathcal{I}_h \psi$ may not belong to the finite element space K_h . Following the work of Chen and Nocketto [18], we choose $\psi_h = P_h(\min\{\mathcal{I}_h \psi, \chi\})$. Hence, $\psi_h \in K_h$ and

$$\psi_h(x_i) = \min\{\mathcal{I}_h \psi(x_i), \chi(x_i)\} \quad \forall i \in N_h. \quad (30)$$

The following inequality, derived by Chen and Nochetto [18, Section 5], is key to our analysis. It is seen from Remark 4.1 and (30) that

$$0 \leq \mathcal{I}_h \psi(x_i) - \psi_h(x_i) \leq (\mathcal{I}_h \psi(x_i) - \chi(x_i))_+ \leq (\mathcal{I}_h \chi(x_i) - \chi(x_i))_+,$$

hence,

$$|\psi_h(x_i) - \mathcal{I}_h \psi(x_i)| \leq |\chi(x_i) - \mathcal{I}_h \chi(x_i)|.$$

Since we assumed that $\chi \in X_h$, we have

$$\begin{aligned} |\chi(x_i) - \mathcal{I}_h \chi(x_i)| &= \frac{1}{|(1, \zeta_i)|} \left| \int_{\omega_i} (\chi(x_i) - \chi) \zeta_i \, dx \right| \\ &= \frac{1}{|(1, \zeta_i)|} \left| \int_{\omega_i} \left(\chi(x_i) - \sum_{j: x_j \in \bar{\omega}_i} \chi(x_j) \zeta_j \right) \zeta_i \, dx \right| \\ &= \frac{1}{|(1, \zeta_i)|} \left| \sum_{j: x_j \in \bar{\omega}_i} \int_{\omega_i} (\chi(x_i) - \chi(x_j)) \zeta_j \zeta_i \, dx \right| \\ &= \frac{1}{|(1, \zeta_i)|} \left| \sum_{j: x_j \in \bar{\omega}_i} (\chi(x_i) - \chi(x_j)) \int_{\omega_i} \zeta_j \zeta_i \, dx \right|, \end{aligned}$$

which can be easily computed using the mass matrix. We therefore define

$$osc_h(\chi; \omega_i) := \frac{1}{|(1, \zeta_i)|} \left| \sum_{j: x_j \in \bar{\omega}_i} (\chi(x_i) - \chi(x_j)) \int_{\omega_i} \zeta_j \zeta_i \, dx \right|, \quad (31)$$

to obtain

$$\begin{aligned} &|\partial_v J(u_h; v_h, \psi_h - \mathcal{I}_h \psi)| \\ &\lesssim \sum_{i \in N_h^c} \left[\sum_{T \subseteq \omega_i} h_T^{N/2} \|q\|_{L^2(T)} + \varepsilon \sum_{e \subset \omega_i \setminus \partial \omega_i} h_e^{N-1} \llbracket \nabla v_h \rrbracket_e \right] osc_h(\chi; \omega_i) \\ &\lesssim \sum_{\substack{T \in \mathcal{T}_h: \\ T \subseteq \mathcal{C}_h(v_h)}} \sum_{i: x_i \in \bar{T}} \left[h_T^{N/2} \|q\|_{L^2(T)} + \varepsilon \sum_{\substack{e \subseteq \partial T \setminus \partial \mathcal{C}_h(v_h): \\ x_i \in \bar{e}}} h_e^{N-1} \llbracket \nabla v_h \rrbracket_e \right] osc_h(\chi; \omega_i), \end{aligned}$$

We conclude the proof by defining

$$|\nu_T^1(u_h, v_h)|^2 := \sum_{i: x_i \in \bar{T}} h_i^2 \|q - \bar{q}_i\|_{L^2(\omega_i)}^2 + 4\varepsilon^2 \sum_{e \subseteq \partial T} h_e \|\llbracket \nabla v_h \rrbracket_e\|_{L^2(e)}^2, \quad (32)$$

$$|\nu_T^2(u_h, v_h)|^2 := \sum_{i: x_i \in \bar{T}} \left[h_T^{N/2} \|q\|_{L^2(T)} + \varepsilon \sum_{\substack{e \subseteq \partial T \setminus \partial \mathcal{C}_h(v_h): \\ x_i \in \bar{e}}} h_e^{N-1} \llbracket \nabla v_h \rrbracket_e \right] osc_h(\chi; \omega_i), \quad (33)$$

and

$$|\nu_T(u_h, v_h)|^2 := \begin{cases} |\nu_T^1(u_h, v_h)|^2 + |\nu_T^2(u_h, v_h)|^2, & \text{if } T \subseteq \mathcal{C}_h(v_h), \\ |\nu_T^1(u_h, v_h)|^2. & \text{if } T \subseteq \mathcal{N}_h(v_h). \end{cases}$$

□

For all $T \in \mathcal{T}_h$ we use $\mu_T(u_h, v_h)$ and $\nu_T(u_h, v_h)$ as local refinement indicator functions for u_h and v_h , respectively. Note that

$$\begin{aligned} \|\partial_u J(u_h, v_h)\|_{(H_D^1(\Omega))^*} &\lesssim \left[\sum_{T \in \mathcal{T}_h} |\mu_T(u_h, v_h)|^2 \right]^{1/2}, \quad \text{and} \\ \sup_{\psi \in K} \frac{\partial_v J(v_h; u_h, v_h - \psi)}{\|\psi\|_{H^1(\Omega)} + 1} &\lesssim \left[\sum_{T \in \mathcal{T}_h} |\nu_T(u_h, v_h)|^2 \right]^{1/2}. \end{aligned}$$

4.3. Adaptive Algorithm

We now state the adaptive algorithm. It has a similar structure to the second adaptive algorithm proposed in [15] for the minimization of the standard Ambrosio–Tortorelli functional. The user-specified tolerances REFTOL_u and REFTOL_v determine when to halt the refinement loops with respect to u and v , respectively. The *marking parameter* θ is a fixed number lying in the interval $(0, 1]$. Within each alternating minimization step $n \in \{m/2 : m \in \mathbb{N}\}$ we denote the mesh at the j th level of refinement by \mathcal{T}_j^n and the associated mesh size $h_j^n := \max_{T \in \mathcal{T}_j^n} \text{diam}(T)$, for all $j \in \mathbb{N}$.

Adaptive Algorithm

1. Input: Initial crack field v^1 and initial mesh $\mathcal{T}^{1/2}$.
2. Alternating minimization loop: For $n = 1, 2, \dots$
 - (a) Set $\mathcal{T}_1^n = \mathcal{T}^{n-1/2}$
 - (b) Mesh refinement loop: For $j = 1, 2, \dots$
 - Compute $u_j^n := \argmin \{J(z, v^n) : z \in X_{h_j^n}^g\}$;
 - If $[\sum_{T \in \mathcal{T}_j^n} |\mu_T(u_j^n, v^n)|^2]^{1/2} > \text{REFTOL}_u$,
 - Find the smallest set $M_j \subseteq \mathcal{T}_j^n$ such that $\sum_{T \in M_j} |\mu_T(u_j^n, v^n)|^2 \geq \theta \sum_{T \in \mathcal{T}_j^n} |\mu_T(u_j^n, v^n)|^2$;
 - Refine elements in M_j to obtain the new mesh \mathcal{T}_{j+1}^n .
 - Repeat until $[\sum_{T \in \mathcal{T}_j^n} |\mu_T(u_j^n, v^n)|^2]^{1/2} \leq \text{REFTOL}_u$.
 - (c) Set $u^n = u_j^n$, $\mathcal{T}^n = \mathcal{T}_j^n$ and $\mathcal{T}_1^{n+1/2} = \mathcal{T}^n$.
 - (d) Mesh refinement loop: For $j = 1, 2, \dots$
 - Compute $v_j^{n+1} \in \argmin \{J(u^n, z) : z \in K_{h_j^{n+1/2}}\}$;
 - If $[\sum_{T \in \mathcal{T}_j^{n+1/2}} |\nu_T(u^n, v_j^{n+1})|^2]^{1/2} > \text{REFTOL}_v$,
 - Find the smallest set $M_j \subseteq \mathcal{T}_j^{n+1/2}$ such that $\sum_{T \in M_j} |\nu_T(u^n, v_j^{n+1})|^2 \geq \theta \sum_{T \in \mathcal{T}_j^{n+1/2}} |\nu_T(u^n, v_j^{n+1})|^2$;
 - Refine elements in M_j to obtain the new mesh $\mathcal{T}_{j+1}^{n+1/2}$.
 - Repeat until $[\sum_{T \in \mathcal{T}_j^{n+1/2}} |\nu_T(u^n, v_j^{n+1})|^2]^{1/2} \leq \text{REFTOL}_v$.
 - (e) Set $v^{n+1} = v_j^{n+1}$ and $\mathcal{T}^{n+1/2} = \mathcal{T}_j^{n+1/2}$;
 - (f) Repeat steps (a) to (e) until $\|v^{n+1} - v^n\|_{L^\infty(\Omega)} < \text{VTOL}$.
3. Set $u_h(t_k) = u^n$ and $v_h(t_k) = v^{n+1}$.

We reiterate the comment made in Section 3.3 that, as currently stated, the algorithm is not well-defined since the v -minimization problem in Step 2(d) may not have a unique minimizer. This will not affect the convergence

analysis of the algorithm, however, for which it is sufficient to compute any minimizer. We therefore postpone our presentation of a specific minimization algorithm for v until Section 5 and begin with a convergence analysis of the Adaptive Algorithm, for which it is useful to consider the following modification.

Adaptive Iteration:

In step n of the Adaptive Algorithm, we replace REFTOL_u and REFTOL_v by REFTOL_u^n and REFTOL_v^n , respectively, and require that $\text{REFTOL}_u^n \rightarrow 0$ and $\text{REFTOL}_v^n \rightarrow 0$ as $n \rightarrow \infty$. Furthermore, we remove the termination condition 2(f) and make the following assumption:

Steps (b) and (d) in the Adaptive Algorithm and Adaptive Iteration terminate in a finite number of iterations. (B)

4.4. Preliminaries

We now state two lemmas that will be useful in the convergence analysis of Section 4.5.

Lemma 4.5. *The sequence $((u^n, v^n))_{n=1}^\infty \subseteq H_g^1(\Omega) \times K$ generated by the Adaptive Iteration is a bounded sequence in $(H^1(\Omega))^m \times H^1(\Omega)$.*

Proof. Let $((u^n, v^n))_{n=1}^\infty \subseteq H_g^1(\Omega) \times K$ be the sequence generated by the Adaptive Iteration, then $(J(u^n, v^n))_{n=1}^\infty$ is a bounded sequence in \mathbb{R} . Since

$$\begin{aligned} J(u^n, v^n) &= \int_{\Omega} \left[(F(v^n) + \eta) A \nabla u^n : \nabla u^n + \varepsilon^{-1} G(v^n) + \varepsilon |\nabla v^n|^2 \right] dx \\ &\geq \eta \|A \nabla u^n : \nabla u^n\|_{L^1(\Omega)} + \varepsilon \|\nabla v^n\|_{L^2(\Omega)}^2, \end{aligned}$$

it follows that $(\|\nabla v^n\|_{L^2(\Omega)})_{n=1}^\infty$ and $(\|A \nabla u^n : \nabla u^n\|_{L^1(\Omega)})_{n=1}^\infty$ are bounded sequences in \mathbb{R} . We also have that $0 \leq v^n(x) \leq 1$ for almost every $x \in \Omega$, which implies that $(\|v^n\|_{L^2(\Omega)})_{n=1}^\infty$ is bounded. Therefore, $(v^n)_{n=1}^\infty$ is bounded in $H^1(\Omega)$.

Using the boundedness of $(\|A \nabla u^n : \nabla u^n\|_{L^1(\Omega)})_{n=1}^\infty$ together with the coercivity and positivity assumptions on A , it can be shown that $(\|\nabla(u^n - g)\|_{L^2(\Omega)})_{n=1}^\infty$ is bounded. Using a variant of the Friedrichs inequality [11, Chapter 2, Section 1.5] and noting that $(u^n - g) \in H_D^1(\Omega)$, for all $n \in \mathbb{N}$, we then have

$$\|u^n\|_{H^1(\Omega)} \leq \|u^n - g\|_{H^1(\Omega)} + \|g\|_{H^1(\Omega)} \leq C_F \|\nabla(u^n - g)\|_{L^2(\Omega)} + \|g\|_{H^1(\Omega)}$$

where $C_F = C_F(\Omega, N) > 0$ is the Friedrichs constant. Therefore, $(\|u^n\|_{H^1(\Omega)})_{n=1}^\infty$ is a bounded sequence. Consequently, $((u^n, v^n))_{n=1}^\infty$ is a bounded sequence in $(H^1(\Omega))^m \times H^1(\Omega)$. \square

Lemma 4.6. *Suppose the sequences $(v_j)_{j=1}^\infty \subset K$ and $(w_j)_{j=1}^\infty \subset L^1(\Omega)$ are such that $v_j \rightarrow v$ in $L^1(\Omega)$ and $w_j \rightarrow w$ in $L^1(\Omega)$ as $j \rightarrow \infty$, for some $v \in K$ and $w \in L^1(\Omega)$. Let $s \in \{1, 2\}$, then*

$$\lim_{j \rightarrow \infty} \int_{\Omega} |f(v) - f(v_j)|^s |w_j| dx = 0 \quad \forall f \in C([0, 1]).$$

Proof. Since $f \in C([0, 1])$,

$$\begin{aligned} \int_{\Omega} |f(v) - f(v_j)|^s |w_j| dx &= \int_{\Omega} |f(v) - f(v_j)|^s |w| dx + \int_{\Omega} |f(v) - f(v_j)|^s (|w| - |w_j|) dx \\ &\leq \int_{\Omega} |f(v) - f(v_j)|^s |w| dx + \|f(v) - f(v_j)\|_{L^\infty(\Omega)}^s \int_{\Omega} |w - w_j| dx. \end{aligned}$$

The strong convergence $w_j \rightarrow w$ in $L^1(\Omega)$ as $j \rightarrow \infty$, therefore implies

$$\limsup_{j \rightarrow \infty} \int_{\Omega} |f(v) - f(v_j)|^s |w_j| \, dx \leq \limsup_{j \rightarrow \infty} \int_{\Omega} |f(v) - f(v_j)|^s |w| \, dx.$$

Let $(v_{j_k})_{k=1}^{\infty}$ be a subsequence of $(v_j)_{j=1}^{\infty}$ such that

$$\lim_{k \rightarrow \infty} \int_{\Omega} |f(v) - f(v_{j_k})|^s |w| \, dx = \limsup_{j \rightarrow \infty} \int_{\Omega} |f(v) - f(v_j)|^s |w| \, dx,$$

and $v_{j_k} \rightarrow v$ a.e. in Ω . Using Lebesgue's Dominated Convergence Theorem [35, Section 5.2] and the continuity of f , we have $\lim_{k \rightarrow \infty} \int_{\Omega} |f(v) - f(v_{j_k})|^s |w| \, dx = 0$ and hence $\limsup_{j \rightarrow \infty} \int_{\Omega} |f(v) - f(v_j)|^s |w| \, dx = 0$. It thus follows that $\lim_{j \rightarrow \infty} \int_{\Omega} |f(v) - f(v_j)|^s |w_j| \, dx = 0$. \square

4.5. Convergence Analysis

The main result of this section is established in Theorem 4.9; the result implies that the sequence $((u^n, v^n))_{n=1}^{\infty}$ computed by the Adaptive Iteration, under Assumption (B), converges to a critical point of J . Before showing this result we first establish two lemmas concerning the convergence of the partial derivatives of J .

Lemma 4.7. *Suppose that there exists a sequence $((u_j, v_j))_{j=1}^{\infty} \subset H_g^1(\Omega) \times K$ and $(u, v) \in H_g^1(\Omega) \times K$ such that $(u_j, v_j) \rightharpoonup (u, v)$ in $(H^1(\Omega))^N \times H^1(\Omega)$. Suppose also that $((u_j, v_j))_{j=1}^{\infty}$ satisfies*

$$\partial_u J(v_j; u_j, \varphi) \leq \mu_j \|\nabla \varphi\|_{L^2(\Omega)} \quad \forall \varphi \in H_D^1(\Omega), \quad (34)$$

for some $\mu_j \in \mathbb{R}_{\geq 0}$ with $\mu_j \rightarrow 0$ as $j \rightarrow \infty$.

Then, u and v satisfy

$$\partial_u J(v; u, \varphi) = 0 \quad \forall \varphi \in H_D^1(\Omega),$$

and $u_j \rightarrow u$ strongly in $(H^1(\Omega))^N$ as $j \rightarrow \infty$.

Proof.

Step 1. $\partial_u J(v; u, \varphi) = 0$ for all $\varphi \in H_D^1(\Omega)$:

Fixing $\varphi \in H_D^1(\Omega)$ we have

$$\begin{aligned} \partial_u J(v; u, \varphi) &= 2 \int_{\Omega} (F(v) + \eta) A \nabla u : \nabla \varphi \, dx \\ &= 2 \int_{\Omega} (F(v) + \eta) A \nabla (u - u_j) : \nabla \varphi \, dx + 2 \int_{\Omega} (F(v_j) + \eta) A \nabla u_j : \nabla \varphi \, dx \\ &\quad + 2 \int_{\Omega} (F(v) - F(v_j)) A \nabla u_j : \nabla \varphi \, dx \\ &=: R_j + S_j + T_j. \end{aligned}$$

Our aim is to show that R_j , S_j and $T_j \rightarrow 0$ as $j \rightarrow \infty$.

Using the symmetry of the elasticity tensor,

$$\begin{aligned} R_j &= 2 \int_{\Omega} (F(v) + \eta) A \nabla (u - u_j) : \nabla \varphi \, dx \\ &= 2 \int_{\Omega} (F(v) + \eta) A \nabla \varphi : \nabla (u - u_j) \, dx. \end{aligned}$$

Since $\nabla u_j \rightharpoonup \nabla u$ in $(L^2(\Omega))^{m \times N}$ and $(F(v) + \eta)A\nabla\varphi \in L^2(\Omega)$ we have $R_j \rightarrow 0$ as $j \rightarrow \infty$.

Now let us examine S_j ; by (34) we have

$$|S_j| \leq \mu_j \|\nabla\varphi\|_{L^2(\Omega)} \rightarrow 0 \text{ as } j \rightarrow \infty.$$

Finally, we estimate T_j as follows

$$\begin{aligned} |T_j| &\leq 2 \int_{\Omega} |F(v) - F(v_j)| |A\nabla u_j| |\nabla\varphi| \, dx \\ &\leq 2C_B \left(\int_{\Omega} |F(v) - F(v_j)|^2 |\nabla\varphi|^2 \, dx \right)^{1/2} \|\nabla u_j\|_{L^2(\Omega)}, \end{aligned}$$

where C_B is the boundedness constant from (1). As $|\nabla\varphi|^2 \in L^1(\Omega)$, it follows from Lemma 4.6 that $T_j \rightarrow 0$ as $j \rightarrow \infty$. Thus we deduce that $\partial_u J(v; u, \varphi) = 0$ for all $\varphi \in H_D^1(\Omega)$.

Step 2. $\nabla u_j \rightarrow \nabla u$ strongly in $(L^2(\Omega))^{m \times N}$:

Using the coercivity assumption (3) on A we have

$$\begin{aligned} 2C_K\eta \|\nabla u - \nabla u_j\|_{L^2(\Omega)}^2 &\leq 2 \int_{\Omega} (F(v_j) + \eta) A(\nabla u - \nabla u_j) : (\nabla u - \nabla u_j) \, dx \\ &= -\partial_u J(v_j; u_j, u - u_j) + 2 \int_{\Omega} (F(v_j) + \eta) A\nabla u : \nabla(u - u_j) \, dx. \end{aligned}$$

By Step 1 we have $\partial_u J(v; u, u - u_j) = 0$; thus

$$\begin{aligned} 2C_K\eta \|\nabla u - \nabla u_j\|_{L^2(\Omega)}^2 &\leq -\partial_u J(v_j; u_j, u - u_j) + 2 \int_{\Omega} (F(v_j) + \eta) A\nabla u : \nabla(u - u_j) \, dx \\ &\quad - \partial_u J(v; u, u - u_j) \\ &= -\partial_u J(v_j; u_j, u - u_j) + 2 \int_{\Omega} (F(v_j) - F(v)) A\nabla u : (\nabla u - \nabla u_j) \, dx \\ &\leq \mu_j \|\nabla u - \nabla u_j\|_{L^2(\Omega)} \\ &\quad + 2C_B \|(F(v_j) - F(v))\nabla u\|_{L^2(\Omega)} \|\nabla(u - u_j)\|_{L^2(\Omega)}. \end{aligned}$$

In summary,

$$2C_K\eta \|\nabla u - \nabla u_j\|_{L^2(\Omega)} \leq \mu_j + 2C_B \left(\int_{\Omega} |F(v_j) - F(v)|^2 |\nabla u|^2 \, dx \right)^{1/2},$$

and thus, using Lemma 4.6 and $\mu_j \rightarrow 0$ as $j \rightarrow \infty$, it follows that $u_j \rightarrow u$ strongly in $(H^1(\Omega))^N$ as $j \rightarrow \infty$. \square

Lemma 4.8. *Suppose that there exists a sequence $((u_j, v_j))_{j=1}^{\infty} \subset H_g^1(\Omega) \times K$ and $(u, v) \in H_g^1(\Omega) \times K$ such that $u_j \rightarrow u$ strongly in $H^1(\Omega)$ and $v_j \rightharpoonup v$ weakly in $H^1(\Omega)$ as $j \rightarrow \infty$. Suppose also that $((u_j, v_j))_{j=1}^{\infty}$ satisfies*

$$\partial_v J(u_j; v_j, v_j - \psi) \leq \nu_j (\|\psi\|_{H^1(\Omega)} + 1) \quad \forall \psi \in K, \quad (35)$$

for some $\nu_j \in \mathbb{R}_{\geq 0}$ with $\nu_j \rightarrow 0$ as $j \rightarrow \infty$.

Then, $v_j \rightarrow v$ strongly in $H^1(\Omega)$ as $j \rightarrow \infty$. Moreover, u and v satisfy

$$\partial_v J(u; v, v - \psi) \leq 0 \quad \forall \psi \in K.$$

Proof.

Step 1. $\nabla v_j \rightarrow \nabla v$ strongly in $(L^2(\Omega))^N$:

Substituting $\psi = v$ into (35) gives

$$\partial_v J(u_j; v_j, v_j - v) \leq \nu_j(\|v\|_{H^1(\Omega)} + 1).$$

Therefore,

$$\begin{aligned} \int_{\Omega} \left[F'(v_j)(v_j - v) A \nabla u_j : \nabla u_j + \varepsilon^{-1} G'(v_j)(v_j - v) + 2\varepsilon \nabla v_j \cdot \nabla(v_j - v) \right] dx \\ \leq \nu_j(\|v\|_{H^1(\Omega)} + 1), \end{aligned}$$

which implies

$$\begin{aligned} 2\varepsilon \int_{\Omega} |\nabla v_j|^2 dx &\leq \nu_j(\|v\|_{H^1(\Omega)} + 1) + 2\varepsilon \int_{\Omega} \nabla v_j \cdot \nabla v dx \\ &\quad + \varepsilon^{-1} \|G'(v_j)\|_{L^2(\Omega)} \|v - v_j\|_{L^2(\Omega)} \\ &\quad + C_B \|F'(v_j)\|_{L^\infty(\Omega)} \int_{\Omega} |v - v_j| |\nabla u_j|^2 dx. \end{aligned}$$

Recall that $\nu_j \rightarrow 0$, $\nabla v_j \rightharpoonup \nabla v$ in $(L^2(\Omega))^N$ and $v_j \rightarrow v$ in $L^2(\Omega)$ as $j \rightarrow \infty$. Hence, using Lemma 4.6 with $w_j = |\nabla u_j|^2$ and $w = |\nabla u|^2$ it follows that

$$\limsup_{j \rightarrow \infty} \|\nabla v_j\|_{L^2(\Omega)}^2 \leq \|\nabla v\|_{L^2(\Omega)}^2.$$

Hence, using the weak lower semi-continuity of the L^2 -norm, we have

$$\|\nabla v\|_{L^2(\Omega)}^2 \leq \liminf_{j \rightarrow \infty} \|\nabla v_j\|_{L^2(\Omega)}^2 \leq \limsup_{j \rightarrow \infty} \|\nabla v_j\|_{L^2(\Omega)}^2 \leq \|\nabla v\|_{L^2(\Omega)}^2,$$

which implies that $\|\nabla v_j\|_{L^2(\Omega)} \rightarrow \|\nabla v\|_{L^2(\Omega)}$ as $j \rightarrow \infty$. This result together with the weak convergence of $(\nabla v_j)_{j=1}^\infty$ to ∇v in $(L^2(\Omega))^N$ implies the strong convergence of $(\nabla v_j)_{j=1}^\infty$ to ∇v in $(L^2(\Omega))^N$, as $j \rightarrow \infty$. Thus, $(v_j)_{j=1}^\infty$ converges strongly to v in $H^1(\Omega)$ as $j \rightarrow \infty$.

Step 2. $\partial_v J(u; v, v - \psi) \leq 0$ for all $\psi \in K$:

Let $\psi \in K$; then

$$\begin{aligned} &\partial_v J(v; u, v - \psi) \\ &= \int_{\Omega} \left[F'(v_j)(v_j - \psi) A \nabla u_j : \nabla u_j + \varepsilon^{-1} G'(v_j)(v_j - \psi) + 2\varepsilon \nabla v_j \cdot \nabla(v_j - \psi) \right] dx \\ &\quad + \int_{\Omega} [F'(v)(v - \psi) A \nabla u : \nabla u - F'(v_j)(v_j - \psi) A \nabla u_j : \nabla u_j] dx \\ &\quad + \varepsilon^{-1} \int_{\Omega} [G'(v)(v - \psi) - G'(v_j)(v_j - \psi)] dx \\ &\quad + 2\varepsilon \int_{\Omega} [\nabla v \cdot \nabla(v - \psi) - \nabla v_j \cdot \nabla(v_j - \psi)] dx \\ &=: Q_j + R_j + S_j + T_j, \end{aligned} \tag{36}$$

by labelling each of the integrals in turn. We now show that $\limsup_{j \rightarrow \infty} Q_j \leq 0$ and $\lim_{j \rightarrow \infty} R_j, S_j, T_j = 0$.

Using (35), we have

$$Q_j \leq \nu_j(\|\psi\|_{H^1(\Omega)} + 1) \rightarrow 0 \quad \text{as } j \rightarrow \infty.$$

We estimate R_j by

$$\begin{aligned} |R_j| &\leq \int_{\Omega} |F'(v) - F'(v_j)| |v - \psi| |A \nabla u : \nabla u| \, dx + \int_{\Omega} |F'(v_j)(v - v_j)| |A \nabla u : \nabla u| \, dx \\ &\quad + \int_{\Omega} |F'(v_j)(v_j - \psi)| |A \nabla u : \nabla u - A \nabla u_j : \nabla u_j| \, dx \\ &\leq \|v - \psi\|_{L^\infty(\Omega)} \int_{\Omega} |F'(v) - F'(v_j)| |A \nabla u : \nabla u| \, dx \\ &\quad + \|F'(v_j)\|_{L^\infty(\Omega)} \int_{\Omega} |v - v_j| |A \nabla u : \nabla u| \, dx \\ &\quad + C_B \|F'(v_j)\|_{L^\infty(\Omega)} \|v_j - \psi\|_{L^\infty(\Omega)} \|\nabla u - \nabla u_j\|_{L^2(\Omega)} \|\nabla u + \nabla u_j\|_{L^2(\Omega)}. \end{aligned}$$

Since $v, \psi, (F'(v_j))_{j=1}^\infty$ and $(v_j)_{j=1}^\infty$ are bounded in $L^\infty(\Omega)$, it therefore follows from Lemma 4.6 and the strong convergence $\nabla u_j \rightarrow \nabla u$ in $(L^2(\Omega))^{m \times N}$ that $R_j \rightarrow 0$ as $j \rightarrow \infty$.

Next, let us consider S_j ,

$$\begin{aligned} |S_j| &\leq \varepsilon^{-1} \int_{\Omega} |G'(v) - G'(v_j)| |v - \psi| \, dx + \varepsilon^{-1} \int_{\Omega} |G'(v_j)| |v - v_j| \, dx \\ &\leq \varepsilon^{-1} \sup_{0 \leq z \leq 1} |G''(z)| \|v - v_j\|_{L^2(\Omega)} \|v - \psi\|_{L^2(\Omega)} + \varepsilon^{-1} \|G'(v_j)\|_{L^2(\Omega)} \|v - v_j\|_{L^2(\Omega)}. \end{aligned}$$

Since $v_j \rightarrow v$ in $(L^2(\Omega))^N$, it follows that $S_j \rightarrow 0$ as $j \rightarrow \infty$.

Finally, the strong convergence $\nabla v_j \rightarrow \nabla v$ in $(L^2(\Omega))^N$ implies that $T_j \rightarrow 0$ as $j \rightarrow \infty$. \square

Theorem 4.9. *Let $((u_n, v_n))_{n=1}^\infty \subset H_g^1(\Omega) \times K$ be the sequence generated by the Adaptive Iteration under Assumption (B).*

Then, there exists a subsequence $((u_{n_j}, v_{n_j}))_{j=1}^\infty$ of $((u_n, v_n))_{n=1}^\infty$ and $(u, v) \in H_g^1(\Omega) \times K$, such that $u_{n_j} \rightarrow u$ strongly in $(H^1(\Omega))^m$ and $v_{n_j} \rightarrow v$ strongly in $H^1(\Omega)$ as $j \rightarrow \infty$. In addition, u and v satisfy

$$\partial_u J(v; u, \varphi) = 0 \quad \forall \varphi \in H_D^1(\Omega), \quad (37)$$

$$\partial_v J(u; v, v - \psi) \leq 0 \quad \forall \psi \in K, \quad (38)$$

that is, (u, v) is a critical point of J in $H_g^1(\Omega) \times K$.

Proof.

Step 1. Existence of convergent subsequences of $((u_n, v_n))_{n=1}^\infty$:

It follows from Lemma 4.5 that the sequence $((u_n, v_n))_{n=1}^\infty$ is bounded in $(H^1(\Omega))^m \times H^1(\Omega)$. Since $H^1(\Omega)$ is a Hilbert space, there exists a subsequence $((u_{n_j}, v_{n_j}))_{j=1}^\infty$ such that

$$(u_{n_j}, v_{n_j}) \rightharpoonup (u, v) \quad \text{in } (H^1(\Omega))^m \times H^1(\Omega) \text{ as } j \rightarrow \infty,$$

for some $(u, v) \in (H^1(\Omega))^m \times H^1(\Omega)$. Since $H_g^1(\Omega)$ and K are convex closed subsets of $H^1(\Omega)$ they are both weakly closed [5, Proposition 2.5]. Hence, $(u, v) \in H_g^1(\Omega) \times K$.

Upon extracting further subsequences we may assume, without loss of generality, that $u_{n_j-1} \rightharpoonup u'$ and $v_{n_j-1} \rightharpoonup v'$ weakly in $H^1(\Omega)$ for some $u' \in H_g^1(\Omega)$ and $v' \in K$.

Step 2. $\nabla u_{n_j-1} \rightarrow \nabla u'$ strongly in $(L^2(\Omega))^{m \times N}$:

Note that

$$\partial_u J(v_{n_j-1}; u_{n_j-1}, \varphi) \leq \mu_{n_j-1} \|\nabla \varphi\|_{L^2(\Omega)} \quad \forall \varphi \in H_D^1(\Omega),$$

with $\mu_{n_j-1} \rightarrow 0$ as $j \rightarrow \infty$. Note also that $(u_{n_j-1}, v_{n_j-1}) \rightarrow (u', v')$ in $H^1(\Omega) \times H^1(\Omega)$. Therefore, it follows from Lemma 4.7 that $\nabla u_{n_j-1} \rightarrow \nabla u'$ in $(L^2(\Omega))^{m \times N}$ as $j \rightarrow \infty$.

Step 3. $\partial_v J(u'; v, v - \psi) \leq 0$ for all $\psi \in K$ and $\nabla v_{n_j} \rightarrow \nabla v$ in $(L^2(\Omega))^N$:

Since

$$\partial_v J(u_{n_j-1}; v_{n_j}, v_{n_j} - \psi) \leq \nu_{n_j} (\|\psi\|_{H^1(\Omega)} + 1),$$

with $\nu_{n_j} \rightarrow 0$ as $j \rightarrow \infty$ and $\nabla u_{n_j-1} \rightarrow \nabla u'$ in $L^2(\Omega)$, it follows from Lemma 4.8 that

$$\partial_v J(u'; v, v - \psi) \leq 0 \quad \forall \psi \in K,$$

and $\nabla v_{n_j} \rightarrow \nabla v$ in $(L^2(\Omega))^N$ as $j \rightarrow \infty$.

Step 4. $\partial_u J(v; u, \varphi) = 0$ for all $\varphi \in H_D^1(\Omega)$ and $\nabla u_{n_j} \rightarrow \nabla u$ in $(L^2(\Omega))^{N \times N}$:

Noting that

$$\partial_u J(v_{n_j}; u_{n_j}, \varphi) \leq \mu_{n_j} \|\nabla \varphi\|_{L^2(\Omega)} \quad \forall \varphi \in H_D^1(\Omega),$$

with $\mu_{n_j} \rightarrow 0$ as $j \rightarrow \infty$, it follows from Lemma 4.7 that

$$\partial_u J(v; u, \varphi) = 0 \quad \forall \varphi \in H_D^1(\Omega),$$

and $\nabla u_{n_j} \rightarrow \nabla u$ in $(L^2(\Omega))^{N \times N}$ as $j \rightarrow \infty$.

Step 5. $u' = u$:

Noting that $(J(u_n, v_n))_{n=1}^\infty$ is a nonincreasing sequence, we have

$$J(u', v) = \lim_{j \rightarrow \infty} J(u_{n_j-1}, v_{n_j}) \leq \lim_{j \rightarrow \infty} J(u_{n_j-1}, v_{n_j-1}) = J(u, v).$$

Since u is a critical point of the strictly convex map $\tilde{u} \mapsto J(\tilde{u}, v)$ it is its unique minimizer. Therefore, $J(u', v) = J(u, v)$ and $u' = u$; hence, (u, v) is a critical point of J . \square

Remark 4.10. We conclude this section with a remark concerning the effect of using a quadrature scheme to evaluate J , as discussed in Remark 3.1. We see two major consequences of using such a scheme; firstly, the residual estimates would contain an extra term accounting for the variational crime committed by the inexact integration. Secondly, if $((u^n, v^n))_{n=1}^\infty$ is the sequence produced by the Adaptive Iteration (using quadrature) it does not immediately hold that $J(u^n, v^n)$ is a nonincreasing sequence; therefore, Step 5 in the proof of Theorem 4.9 requires modification. At present, it is unclear to us how to achieve an appropriate modification of Step 5 and we are thus currently unable to prove that the Adaptive Iteration converges to a critical point when a quadrature scheme is used to evaluate J .

5. GRADIENT PROJECTION ALGORITHM

The Adaptive Algorithm requires us to find a local minimizer of the generalised Ambrosio–Tortorelli functional with respect to each variable separately. Although it is a straightforward computation to minimize J

with respect to u (since J is quadratic in u) the minimization with respect to v is more involved. This is, firstly, because of the fact that J may be nonconvex in v and, secondly, as a result of the bound constraints on v . In this section we present an algorithm that may be used to compute a local minimizer of the v minimization problem.

We consider the minimization of J with respect to v_h , for fixed u_h , on a fixed mesh \mathcal{T}_h . Let

$$\chi(x) = \sum_{i \in N_h} \chi_i \zeta_i(x) \quad \text{and} \quad \mathcal{K} := \prod_{i=1}^{|N_h|} [0, \chi_i].$$

For all $\mathbf{w} \in \mathbb{R}^{|N_h|}$, with $\mathbf{w} = (w_1, \dots, w_{|N_h|})$, we define

$$\mathcal{J}(\mathbf{w}) := J\left(u_h, \sum_{i=1}^{|N_h|} w_i \zeta_i(x)\right).$$

The discrete bound-constrained minimization problem for v can now be written in the following form: Find $\mathbf{v} \in \mathcal{K}$, such that

$$\mathbf{v} \in \operatorname{argmin} \{\mathcal{J}(\hat{\mathbf{v}}) : \hat{\mathbf{v}} \in \mathcal{K}\}.$$

Let $\nabla \mathcal{J}(\mathbf{v})$ and $\mathcal{H}(\mathbf{v})$ denote the gradient and Hessian of $\mathcal{J}(\mathbf{v})$, respectively.

Definition 5.1. We call $\mathbf{v} \in \mathcal{K}$ a *critical point* of \mathcal{J} if

$$\nabla \mathcal{J}(\mathbf{v})^T (\mathbf{v} - \mathbf{w}) \leq 0 \quad \text{for all } \mathbf{w} \in \mathcal{K}.$$

We consider two algorithms: the gradient projection algorithm, which can be used for any functions F and G satisfying the conditions set out in Section 1.3 and the projected Newton method for the case when the functions F and G are convex. These two algorithms are natural extensions of the steepest descent algorithm and Newton's method to a bound-constrained minimization problem. Before presenting the algorithms it is useful to introduce the following definitions.

For $\mathbf{v} \in \mathcal{K}$, with $\mathbf{v} = (v_1, \dots, v_{|N_h|})$, and $0 \leq \delta \leq 0.5$ we define the δ -active set

$$\mathcal{A}^\delta(\mathbf{v}) := \{i \in N_h : v_i \leq \delta \text{ or } v_i \geq \chi_i - \delta\}.$$

For $\mathbf{w} \in \mathbb{R}^{|N_h|}$, with $w = (w_1, \dots, w_{|N_h|})$, we define the l_2 projection $\mathcal{P} : \mathbb{R}^{|N_h|} \rightarrow \mathcal{K}$ by

$$\mathcal{P}(\mathbf{w}) := ([\mathcal{P}(\mathbf{w})]_1, \dots, [\mathcal{P}(\mathbf{w})]_{|N_h|})^T,$$

where

$$[\mathcal{P}(\mathbf{w})]_i := \begin{cases} 0, & \text{if } w_i \leq 0, \\ w_i, & \text{if } 0 < w_i < \chi_i, \\ \chi_i, & \text{if } w_i \geq \chi_i, \end{cases} \quad \forall i \in N_h.$$

We also define

$$\hat{\mathbf{w}} := \mathcal{P}(\mathbf{w} - \nabla \mathcal{J}(\mathbf{w})).$$

It can be shown (see [29, Section 5.2]) that $\mathbf{v} \in \mathcal{K}$ is a critical point of \mathcal{J} if, and only if,

$$\mathbf{v} = \mathcal{P}(\mathbf{v} - \lambda \nabla \mathcal{J}(\mathbf{v})) \quad \forall \lambda \geq 0.$$

We will use $|\mathbf{v} - \hat{\mathbf{v}}| \leq \text{TOL}$ as a termination criterion for the two algorithms, where $\text{TOL} > 0$ is a user-specified tolerance.

We first state the gradient projection algorithm. Each iterate $k \in \mathbb{N}$ of the algorithm conducts a line search in the steepest descent direction, projected onto the feasible region, until a sufficient decrease condition is satisfied. The tolerance $\text{TOL} > 0$ and the values $\alpha \in (0, 1)$ and $\beta \in (0, 1)$ are specified by the user.

Gradient Projection Algorithm

1. Input \mathbf{v}^1 ;
2. For $k = 1, 2, \dots$
 - (a) Compute the descent direction $\mathbf{d}^k := -\nabla \mathcal{J}(\mathbf{v}^k)$;
 - (b) Set $j = 0$ and $\mathbf{v}^\lambda = \mathbf{v}^k$;
 - (c) Line search:
 - While $\mathcal{J}(\mathbf{v}^\lambda) - \mathcal{J}(\mathbf{v}^k) \geq -\frac{\alpha}{\lambda} |\mathbf{v}^\lambda - \mathbf{v}^k|^2$;
 - $j = j + 1, \lambda = \beta^j$;
 - $\mathbf{v}^\lambda = \mathcal{P}(\mathbf{v}^k + \lambda \mathbf{d}^k)$;
 - (d) $\mathbf{v}^{k+1} = \mathbf{v}^\lambda$;
 - (e) Repeat steps (a) to (d) until $|\mathbf{v}^{k+1} - \hat{\mathbf{v}}^{k+1}| \leq \text{TOL}$.

Let $(\mathbf{v}^k)_{k=1}^\infty$ be the sequence generated by the gradient projected algorithm (upon removing the termination criterion (e)); then, it can be shown [29] that every limit point of $(\mathbf{v}^k)_{k=1}^\infty$ is a critical point of \mathcal{J} .

In the case when the functions F and G are strictly convex, the Hessian is positive definite and a projected Newton Method may be used. The algorithm uses $-\mathcal{H}_R(\mathbf{v}, \delta)^{-1} \nabla \mathcal{J}(\mathbf{v})$ as a descent direction where $\mathcal{H}_R(\mathbf{v}, \delta)$ is the *reduced Hessian*, which is defined as follows:

$$\mathcal{H}_R(\mathbf{v}, \delta) := \begin{cases} \delta_{ij} & \text{if } i \in \mathcal{A}^\delta(\mathbf{v}) \text{ or } j \in \mathcal{A}^\delta(\mathbf{v}), \\ \mathcal{H}_{ij} & \text{otherwise,} \end{cases}$$

where \mathcal{H}_{ij} is the (i, j) th entry of $\mathcal{H}(\mathbf{v})$ and $\delta \in [0, 0.5]$.

The projected Newton algorithm is stated below for some user-specified values $\text{TOL} > 0$, $\alpha \in (0, 1)$, $\beta \in (0, 1)$ and $\delta \in (0, 0.5]$.

Projected Newton Algorithm

1. Input \mathbf{v}^1 ;
2. For $k = 1, 2, \dots$
 - (a) Compute the descent direction $\mathbf{d}^k = -\mathcal{H}_R(\mathbf{v}^k, \delta)^{-1} \nabla \mathcal{J}(\mathbf{v}^k)$;
 - (b) Set $j = 0$ and $\mathbf{v}^\lambda = \mathbf{v}^k$;
 - (c) Line search:
 - While $\mathcal{J}(\mathbf{v}^\lambda) - \mathcal{J}(\mathbf{v}^k) \geq -\alpha \nabla \mathcal{J}(\mathbf{v}^k)^T (\mathbf{v}^k - \mathbf{v}^\lambda)$;
 - $j = j + 1, \lambda = \beta^j$;
 - $\mathbf{v}^\lambda = \mathcal{P}(\mathbf{v}^k + \lambda \mathbf{d}^k)$;
 - (d) $\mathbf{v}^{k+1} = \mathbf{v}^\lambda$;
 - (e) Repeat steps (a) to (d) until $|\mathbf{v}^{k+1} - \hat{\mathbf{v}}^{k+1}| \leq \text{TOL}$.

Let $(\mathbf{v}^k)_{k=1}^\infty$ be the sequence generated by the projected Newton algorithm (upon removing the termination criterion (e)); if the sequence of condition numbers of the Hessians is bounded, then it can be shown [29] that every limit point of $(\mathbf{v}^k)_{k=1}^\infty$ is a critical point of \mathcal{J} .

Remark 5.2. The gradient projection and projected Newton algorithms are halted after finitely many steps; thus, they do not compute an exact critical point of \mathcal{J} with respect to \mathbf{v} . This is, however, sufficient since for Theorem 4.9 to hold we only require that, at each alternating minimization step $n \in \mathbb{N}$, the solution vector \mathbf{v}

satisfies

$$\nabla \mathcal{J}(\mathbf{v})^T(\mathbf{v} - \mathbf{w}) \leq \delta_n \quad \forall \mathbf{w} \in \mathcal{K},$$

with $\delta_n \rightarrow 0$ as $n \rightarrow \infty$.

In the case where the functions F and G are quadratic it is possible to replace Step 2(c) of the Projected Newton Algorithm with an exact line search, in which a local minimizer of \mathcal{J} is computed, with respect to $\lambda \in \mathbb{R}$, along the piecewise linear path $\mathcal{P}(\mathbf{v}^k + \lambda \mathbf{d}^k)$. We use the line search specified by Nocedal and Wright [33, Section 16.6], which is described next.

At each iterate $k \in \mathbb{N}$, the *breakpoints* are defined to be the values of λ at which one (or more) of the components of $\mathcal{P}(\mathbf{v}^k + \lambda \mathbf{d}^k)$ reaches either of the bound constraints. Letting \mathbf{v}_i^k and \mathbf{d}_i^k denote the i th component of \mathbf{v}^k and \mathbf{d}^k , respectively; the breakpoints can be computed as follows:

$$\bar{\lambda}_i^k = \begin{cases} \frac{(\chi_i - \mathbf{v}_i^k)}{\mathbf{d}_i^k}, & \text{if } \mathbf{d}_i^k > 0, \\ -\frac{\mathbf{v}_i^k}{\mathbf{d}_i^k}, & \text{if } \mathbf{d}_i^k < 0, \\ +\infty, & \text{otherwise,} \end{cases} \quad \forall i \in N_h.$$

Upon ordering the set of breakpoints and removing any duplicate values we denote the remaining values by $\{\lambda_1^k, \dots, \lambda_m^k\}$, where $0 < \lambda_1^k < \lambda_2^k < \dots < \lambda_m^k$. The exact line search then considers each interval $\lambda \in [\lambda_i^k, \lambda_{i+1}^k]$, $i = 1, \dots, m-1$, in turn and determines whether there exists a local minimizer of $\mathcal{J}(\mathbf{v}^k + \lambda \mathbf{d}^k)$ with respect to λ in that interval. This is easily verified since, on each interval, we have an unconstrained minimization problem for a quadratic functional. If a local minimizer is located the line search is halted, otherwise the next interval is examined.

6. COMPUTATIONAL EXAMPLE

The computational examples presented in this section aim to address two questions. Firstly, what is the effect of using a monotonicity constraint on the phase-field variable to impose irreversibility of the crack? Secondly, how does the choice of the functions F and G in the generalised Ambrosio–Tortorelli functional affect the evolution of the crack and the profile of the associated minimizers? In order to focus on these two issues we restrict, for simplicity, the computations to the anti-plane setting taking $N = 2$, $m = 1$ and $A \nabla u : \nabla u = |\nabla u|^2$.

We consider one example for which the evolution of the energy can be computed to high accuracy using Griffith's theory. Let Ω be the two-dimensional rectangular domain $(-1, 1) \times (0, 2.2)$, containing a slit along $\{0\} \times [1.5, 2.2]$. This is shown in Figure 1 (a) where the shaded part $((-1, 0) \cup (0, 1)) \times (2, 2.2)$ is Ω_D . The applied anti-plane displacement $g(x, t)$ is given as follows:

$$g(x, t) = \begin{cases} -t, & \text{on } (-1, 0) \times (2, 2.2), \\ t, & \text{on } (0, 1) \times (2, 2.2), \end{cases} \quad (39)$$

where t is yet to be specified.

Rather than computing on the whole domain Ω we exploit the symmetry of the problem to compute on the half-domain $\bar{\Omega} = (0, 1) \times (0, 2.2)$, shown in Figure 1 (b). The applied displacement g in (39) is appropriately modified as follows:

$$\tilde{g}(x, t) = \begin{cases} 0, & \text{on } \{0\} \times (0, 1.5), \\ t, & \text{on } (0, 1) \times (2, 2.2). \end{cases}$$

We also set $v(x, t) \equiv 1$ on Ω_D , at all times t . This will allow us to use linear functions for both F and G in Section 6.2. The imposition of the boundary condition on v is justified since Ω_D is simply a technical tool that we use to impose the boundary condition for u .

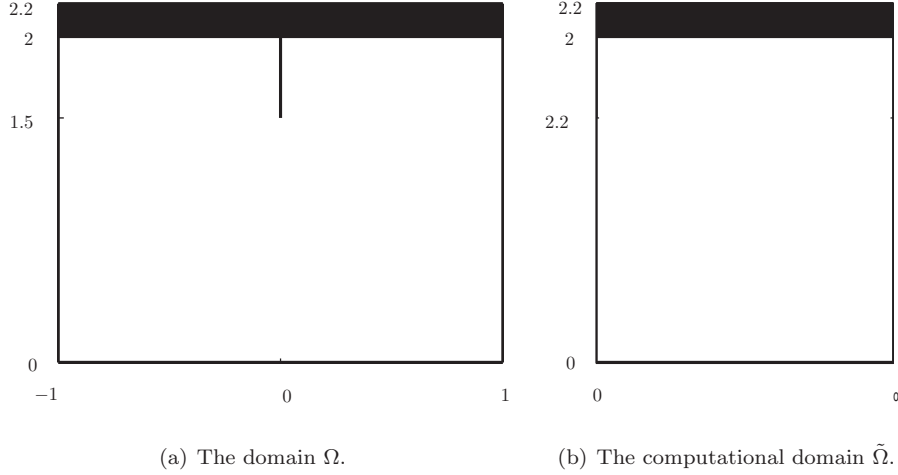


FIGURE 1. The straight crack example.

Since we know, a priori, that the crack path lies along the line $x = 0$, Griffith's criterion [28] can be used to compute the evolution of the crack together with the associated bulk and surface energies. This will be achieved using Algorithm 1 from the paper by Negri and Ortner [32, Page 1914]. In their algorithm the energy release rate is computed using the formula given on Page 1913 of [32], with the bulk energy (for each fixed crack length) computed using an adaptive finite element method. This method allows the energies to be computed to a high degree of accuracy; we will therefore label them as 'exact' and use them as a basis for comparison with our own computational results.

6.1. Implementation of the Irreversibility Condition

We first restrict our attention to the implementation of the irreversibility condition. We will compare the monotonicity condition proposed in this paper with the Dirichlet condition used in [15], which was originally proposed by Bourdin [8]. We refer to the two implementations as the monotonicity implementation and the Dirichlet implementation, respectively.

We fix the functions $F(v) = v^2$ and $G(v) = \frac{1}{4}(1 - v)^2$ (the standard Ambrosio–Tortorelli functional) and the parameters $\varepsilon = 10^{-2}$, $\eta = 10^{-5}$, $\text{VTOL} = 10^{-3}$, $\text{TOL} = 10^{-5}$, $\delta = 10^{-8}$ and $\theta = 0.25$. At each time step the initial crack field v is taken to be the final computed v from the previous time step, with the exception of the first time step where it is taken to be $v \equiv 1$.

We first compare the evolution of the energy of the body, computed using the monotonicity implementation, the Dirichlet implementation, and the exact solution. We use the time discretisation $t = 0.01s$, where $s = 1, \dots, 140$. The Dirichlet implementation uses Algorithm 2 from [15], taking $\text{CRTOL} = 10^{-4}$ and $\text{REFTOL} = 0.05$. The monotonicity implementation uses the Adaptive Algorithm from Section 4.3 with a projected Newton method (with exact line search) taking $\text{MCTOL} = \varepsilon$ and $\text{REFTOL}_u = 0.15$. We take REFTOL_v to be 0.08 at each time step until failure (when the body splits into two pieces) and from this time the tolerance is raised to $\text{REFTOL}_v = 0.1$. This is done to prevent the Adaptive Algorithm over-refining the mesh at times that are physically of no concern.

Figure 2 shows the computed bulk, surface and total energies. The energies computed using the two implementations are very similar; however, we note that the monotonicity implementation computes a smoother evolution of the energies. The number of elements in the mesh at the time of failure are 159815 and 355621 for the Dirichlet and monotonicity implementations, respectively.

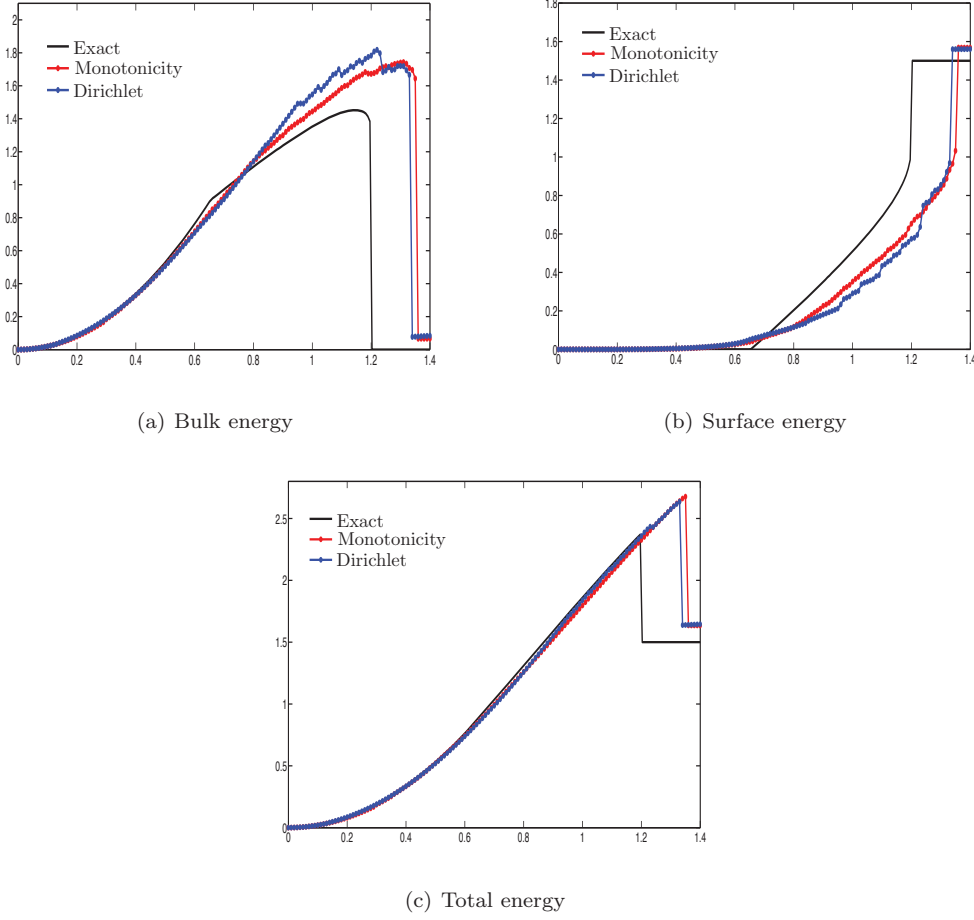


FIGURE 2. A comparison of the bulk, surface and total energies computed using the monotonicity and Dirichlet implementations of the irreversibility condition, with the standard Ambrosio–Tortorelli functional.

Next we consider the effect of changing the value of MCTOL in the monotonicity implementation. In all the computations we take $\text{REFTOL}_u = 0.15$ and $\text{REFTOL}_v = 0.15$. The time discretisation is $t = 0.05s$, where $s = 1, \dots, 36$. Figure 3 shows the computed energies for the values $\text{MCTOL} = 0, \varepsilon, 0.5$ and 1 . Note that the energies are less accurate compared with those in Figure 2 since a lower refinement tolerance for v has been used. Figure 3 shows that, for this example, a large value of MCTOL results in a less accurate solution. The most accurate energies are computed when $\text{MCTOL} = \varepsilon$ and 0 . We believe, however, that taking $\text{MCTOL} = 0$, which corresponds to no enforcement of the irreversibility condition, in experiments for which the applied displacement g is not monotonically increasing in time would not compute such accurate energies. For such examples it is likely that the irreversibility condition would need to be enforced in order to prevent the crack from healing itself when the applied displacement is removed.

Figure 4 compares the final computed v -field for $\text{MCTOL} = \varepsilon$ and 1 . Note that choosing $\text{MCTOL} = 1$ enforces the monotonicity constraint on $v_h(x)$ for all $x \in \Omega$, which is the condition shown by Giacomini [27] to be equivalent to irreversibility of the crack-path in the limit $\varepsilon, \Delta t \rightarrow 0$. Figure 4 demonstrates, however, that in practice this is not a feasible method for imposing irreversibility; it is seen that in the unfractured part of the domain v_h

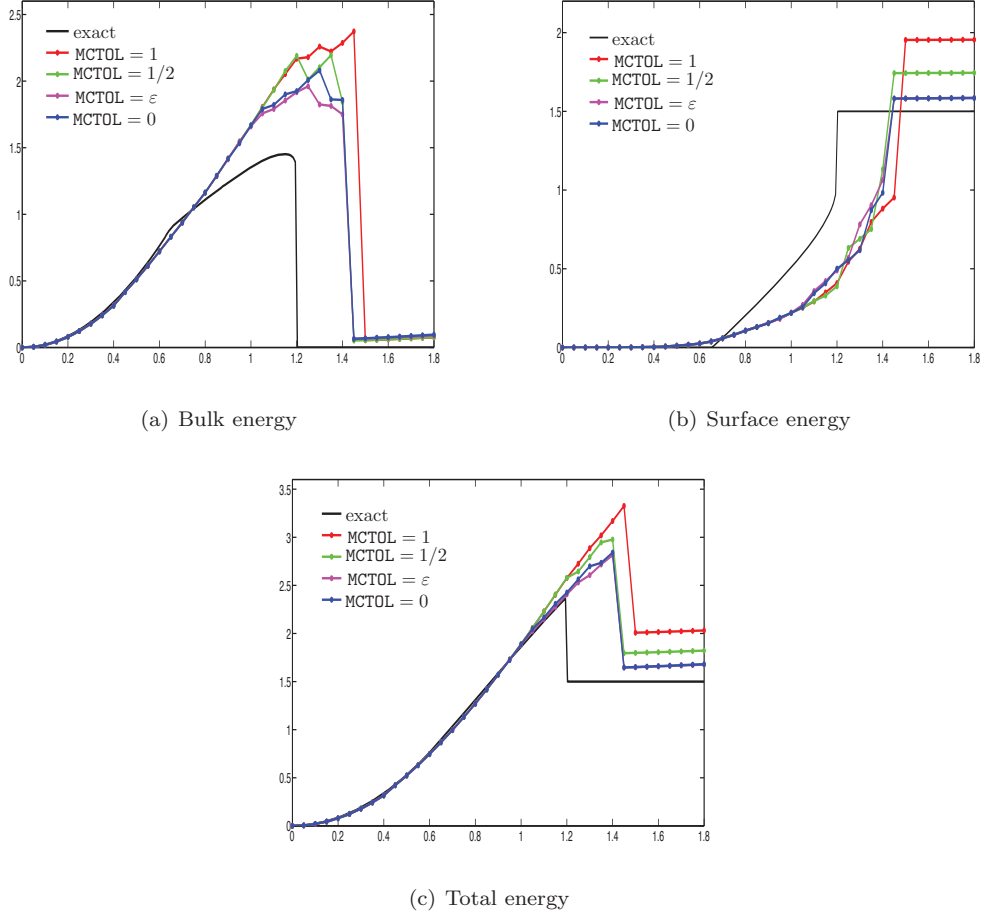


FIGURE 3. A comparison of the bulk, surface and total energies computed using the monotonicity implementation for different values of MCTOL with the standard Ambrosio–Tortorelli functional.

is significantly smaller than one, whilst in the fractured part of the domain the transition layer of v_h does not run straight. These effects are reflected in Figure 3 by the fact that MCTOL = 1 has a greater surface energy than any other value of MCTOL. We believe that these effects occur, since, at each time there is an error in the computed solution arising from the fact that $\varepsilon > 0$. This manifests itself most clearly at early times (before the initial crack starts to propagate) when v_h decreases too much in all parts of the domain. By imposing the monotonicity of the phase-field variable throughout the domain this error is unable to correct itself; hence, the solution remains below one. In contrast, imposing irreversibility only when v_h is sufficiently small allows v_h to increase in the unfractured region at later times. We believe that this is not, purely, a numerical effect and would also occur if the exact solution were computed at each time with $\varepsilon > 0$.

In order to assess how the refinement of the mesh is affected by the obstacle χ we compare the final mesh computed by each value of MCTOL on a subset of the domain close to the crack. This is shown in Figure 5. Recall

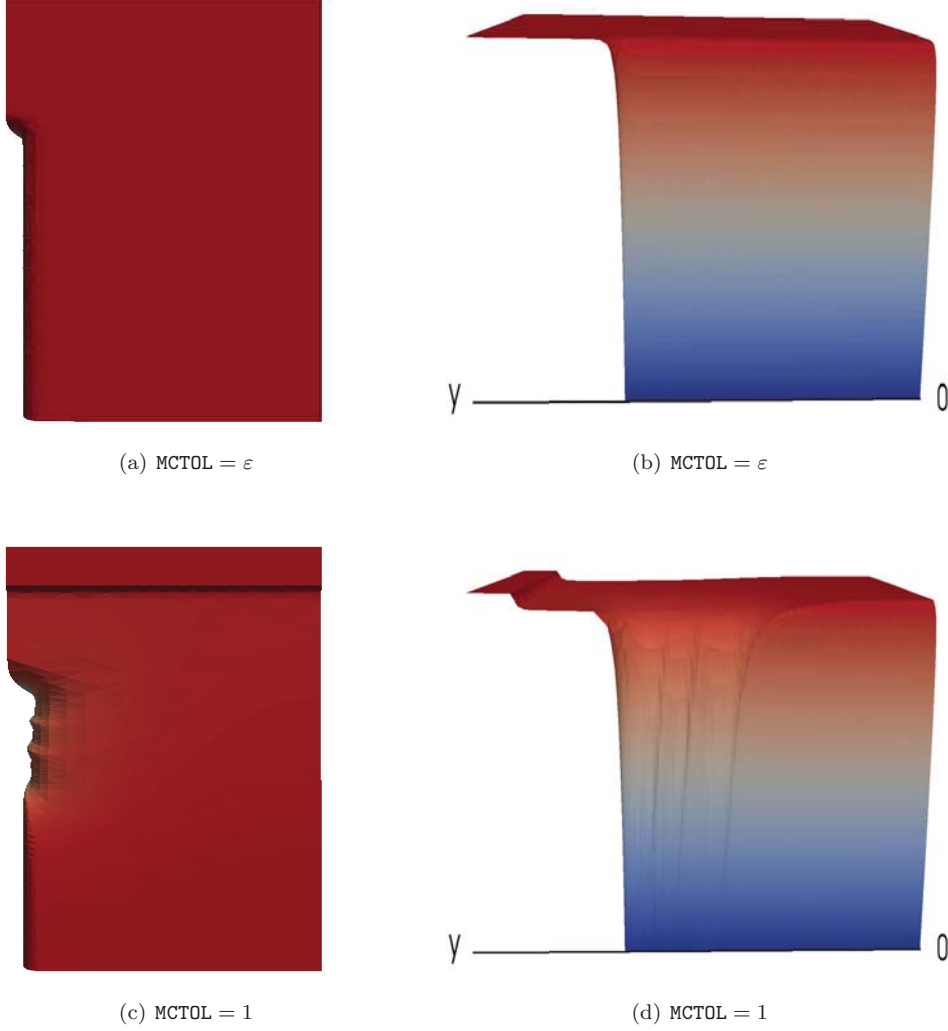


FIGURE 4. A comparison of the final computed v -field for $\text{MCTOL} = \varepsilon$ and $\text{MCTOL} = 1$. Figures (a) and (c) view the v -field from above, projected onto the $x - y$ plane. Figures (b) and (d) show the v -field from the side, projected onto a the $y - z$ plane. The red and blue parts of the domain represent $v = 1$ and $v = 0$, respectively.

that for all elements $T \in \mathcal{T}_h$ the refinement indicator $\nu_T(u_h, v_h)$, associated with v , takes the following form:

$$|\nu_T(u_h, v_h)|^2 := \begin{cases} |\nu_T^1(u_h, v_h)|^2 + |\nu_T^2(u_h, v_h)|^2, & \text{if } T \subseteq \mathcal{C}_h(v_h), \\ |\nu_T^1(u_h, v_h)|^2. & \text{if } T \subseteq \mathcal{N}_h(v_h), \end{cases}$$

where $\nu_T^1(u_h, v_h)$ and $\nu_T^2(u_h, v_h)$ are given in (32) and (33), respectively.

When $\text{MCTOL} = 0$ we have $\chi \equiv 1$, hence the term osc_h in $\nu_T^2(u_h, v_h)$ (see (31)) is zero throughout the domain. This means that the refinement of the mesh is controlled entirely by $\nu_T^1(u_h, v_h)$. However, when $\text{MCTOL} = 0.5$ and ε , at time $t = t_k$, the obstacle χ jumps from $\chi = 1$ to $\chi = v_h(t_{k-1})$ across elements in the

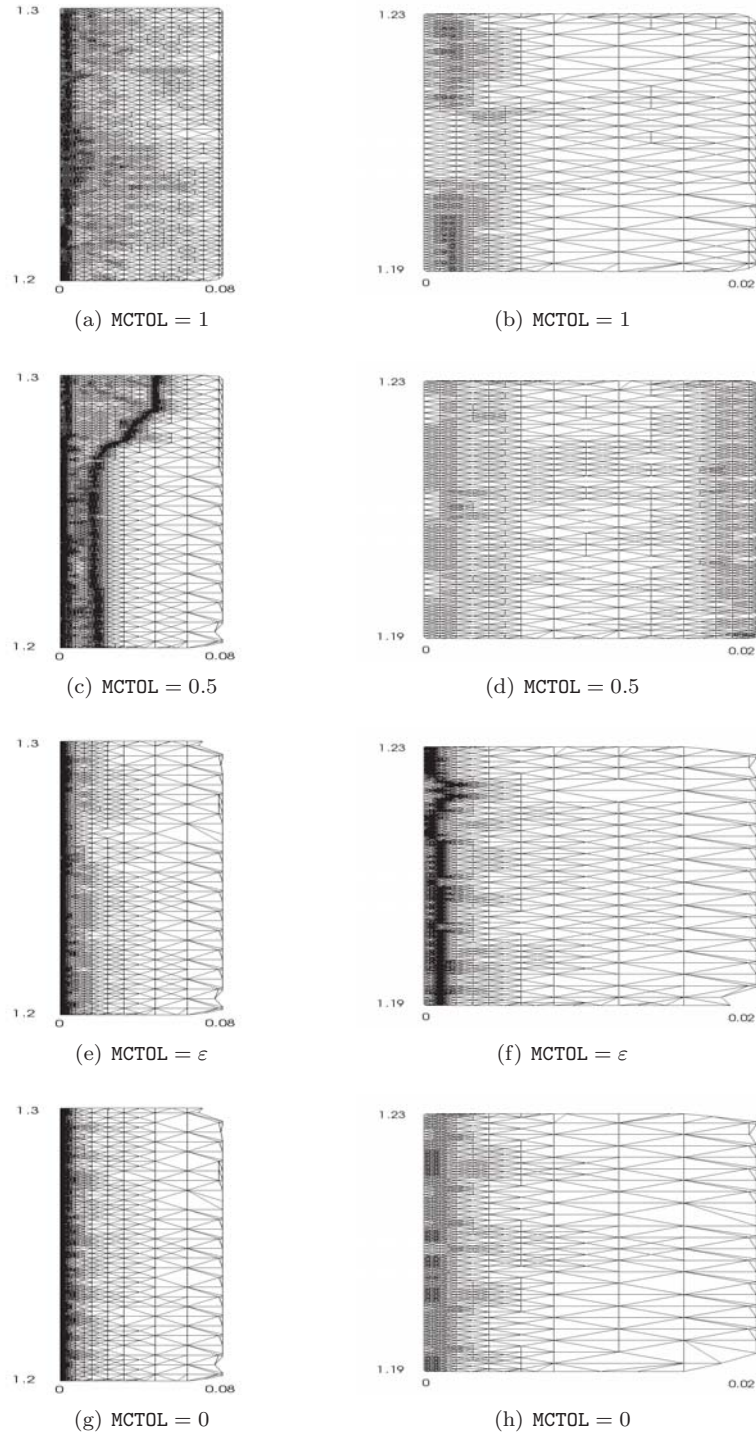


FIGURE 5. A comparison of the final mesh on the subdomains $[0, 0.08] \times [1.2, 1.3]$ and $[0, 0.02] \times [1.19, 1.23]$ computed for $MCTOL = 1, 0.5, \varepsilon$ and 0 . The total number of elements in the final mesh for $MCTOL = 1, 0.5, \varepsilon$ and 0 is 94845, 114292, 255686 and 76147, respectively.

region $v_h(t_{k-1}) \approx \text{MCTOL}$. In this region osc_h is large and hence the mesh experiences a significant amount of refinement due to $\nu_T^2(u_h, v_h)$. This accounts for the refinement seen in Figures 5 (b) and (g), in which elements are refined near $v_h(t_{k-1}) = \text{MCTOL}$. Finally, when $\text{MCTOL} = 1$ we have $\chi = v_h(t_{k-1})$ at time $t = t_k$. Thus, the refinement indicator $\nu_T^2(u_h, v_h)$ is in general nonzero on the whole domain, however, it is small since χ does not experience any ‘large’ jumps across elements. Hence, the refinement is dominated by $\nu_T^1(u_h, v_h)$ as with $\text{MCTOL} = 0$. These refinement patterns are reflected in the number of elements that are contained in the final mesh, which is 94845, 114292, 485049 and 76147 for $\text{MCTOL} = 1, 0.5, \varepsilon$ and 0, respectively. We therefore see that the mesh is over-refined when $\text{MCTOL} = 0.5$ and ε , since the refinement does not take place to increase the resolution of the minimizer but occurs instead because of a jump in the obstacle χ .

We conclude that, forcing v to be a monotonically decreasing function (in time) throughout the domain, which was shown by Giacomini to be equivalent to the irreversibility of the crack in the limit $\varepsilon, \Delta t \rightarrow 0$, is not a feasible method in practice. However, implementing a monotonicity condition on v in a subset of the domain in which v is sufficiently small appears promising. It has been seen that the resulting energy is comparable to that computed using the Dirichlet implementation of the previous chapter. However, the present refinement indicator function for v produces an over-refinement of the mesh for nonzero values of MCTOL , which are significantly smaller than 1 due to a jump in the obstacle χ . Hence, the efficiency of the adaptivity could be improved by considering alternative methods for estimating the residual $\partial_v J(u_h; v_h, v_h - \psi)$.

6.2. Alternative Functionals

In this second set of numerical experiments we compute the evolution of the body with four different generalised Ambrosio–Tortorelli functionals. Let J_{ij} , $i, j = 1, 2$, be the functional J with $F(v) = F_i(v)$, $i = 1, 2$ and $G(v) = G_j(v)$, $j = 1, 2$, where

$$F_1(v) = v, \quad F_2(v) = v^2, \quad G_1(v) = \frac{9}{64}(1-v) \quad \text{and} \quad G_2(v) = \frac{1}{4}(1-v)^2.$$

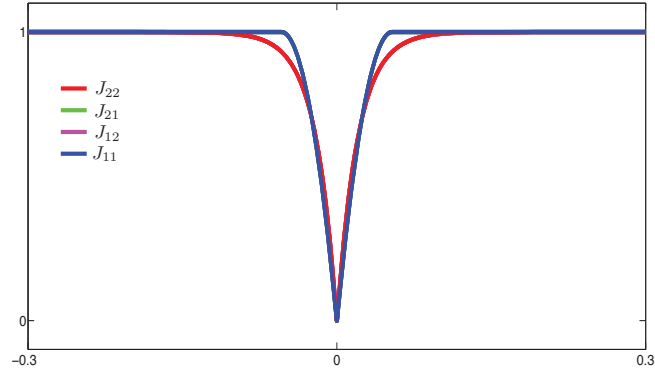
The coefficients $\frac{9}{64}$ and $\frac{1}{4}$ in $G_1(v)$ and $G_2(v)$ ensure that the constant C_S , which is the scaling of the surface energy E_S defined in (6), is equal to one.

To motivate this choice of functions for F and G we present the results of a simple one-dimensional example, which show the profiles of the displacement and phase-field variables across a crack. We consider the domain $\Omega = [-4, 4]$ with an initial mesh containing vertices at $x_i = -4 + (i-1)h$, for $i = 1, \dots, N$, where $N = 1001$ and $h = 8 \times 10^{-3}$. The fixed displacement $u(-4) = 0$ and $u(4) = 2$ is imposed at the two ends of the domain. We only consider the minimization of J_{ij} , $i, j = 1, 2$, at one time and a crack is ‘created’ at $x = 0$ by starting the minimization algorithm with an initial input close to a local minimizer corresponding to a cracked state.

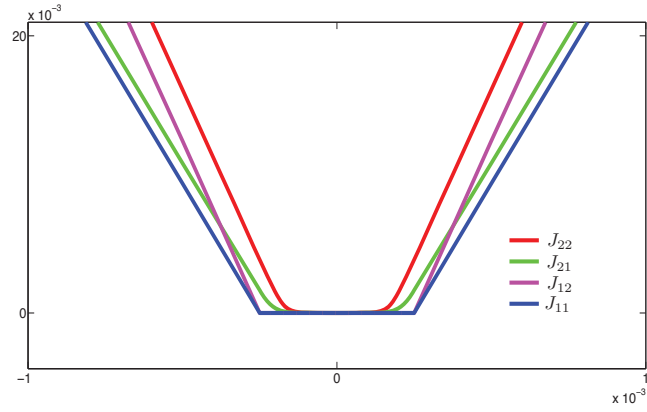
Figure 6 shows the profiles of the phase-field and displacement variables across the crack. We first discuss some of the properties produced by G . Taking $G = G_1$ results in the constraint $v \leq 1$ being enforced away from the crack, that is, $v = 1$ is an active constraint; hence the transition and cracked regions for v are compactly supported and there is a clear distinction between the ‘uncracked’ part of the domain and the transition region. Note that this is not true for $G = G_2$ since $v < 1$ throughout the domain. We therefore hypothesise that, in general, a propagating crack will be less affected by the boundary of the domain with $G = G_1$ than $G = G_2$. We also comment that taking $G = G_1$ produces a transition region for v that is a quadratic function (compared to an exponential function for $G = G_2$); hence, in theory, the phase-field variable can be resolved with fewer elements.

We now discuss some properties produced by the function F . We observe that taking $F = F_1$ results in the constraint $v \geq 0$ being enforced close to the crack, that is, $v = 0$ is an active constraint; hence the cracked region is compactly supported. This is not true for $G = G_2$ since $v > 0$ throughout the domain. The displacement is also affected by the function F . Taking $F = F_1$ produces a profile that is comprised of three almost linear segments. This potentially allows it to be resolved using fewer elements than $F = F_2$.

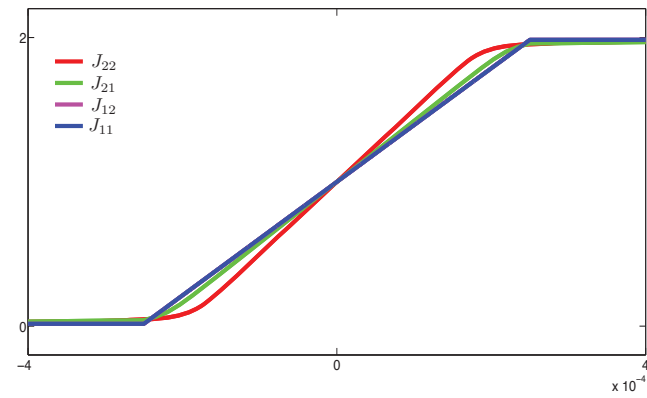
Let us now return to the two-dimensional example presented at the beginning of Section 6. We use the Adaptive Algorithm with the projected Newton and exact line search methods, fixing $\varepsilon = 10^{-2}$, $\eta = 10^{-5}$,



(a) Profile of the phase-field variable. The profiles associated with J_{21} and J_{11} are indistinguishable in this diagram, as are the profiles associated with J_{22} and J_{12} .



(b) Profile of the phase-field variable v near $v = 0$



(c) Profile of the displacement variable near the crack. The profiles associated with J_{12} and J_{11} are indistinguishable in this diagram.

FIGURE 6. A comparison of the phase-field and displacement profiles across a one-dimensional crack.

$\text{VTOL} = 10^{-3}$, $\text{TOL} = 10^{-5}$, $\delta = 10^{-8}$, $\text{REFTOL}_u = 0.15$, $\text{MCTOL} = \varepsilon$ and $\theta = 0.25$. The value of REFTOL_v depends on the choice of functional: for J_{11} and J_{12} we take $\text{REFTOL}_v = 0.4$; for J_{21} we take $\text{REFTOL}_v = 0.08$; and for J_{22} we take $\text{REFTOL}_v = 0.08$ at each time until failure and after this time the tolerance is raised to $\text{REFTOL}_v = 0.1$. These values have been chosen pragmatically to prevent excessively large run-times. In particular, this requires the Adaptive Algorithm to take larger values of REFTOL_v for J_{11} and J_{12} , since these functionals produce a more refined mesh, than J_{21} and J_{22} , for each fixed value of REFTOL_v . The time discretisation is $t = 0.05s$, where $s = 1, \dots, T$ and $T \leq 40$. At each time step the initial crack field v is taken to be the final computed v from the previous time step, with the exception of the first time step where it is taken to be $v \equiv 1$.

Figure 7 shows the evolution of the energy computed for each choice of J . Before the initial crack starts to propagate the energies computed by all four functionals are very similar. However, after the propagation of the initial crack there are significant differences in the energies computed by the four functionals. J_{11} and J_{12} grossly over-estimate the bulk and total energies whilst the computed surface energy is underestimated, which results in a later failure time. The final computed surface energy for J_{11} and J_{12} is greatly over-estimated, however, one nice feature of these functionals is that the final computed bulk energy is much closer to zero. This is because the gradient of u is much closer to zero in the uncracked region for these functionals, as seen in Figure 6 (c) for the one-dimensional example.

In comparison, the two functionals J_{22} and J_{21} compute energies that are much closer to the exact solution, with J_{21} being the more accurate of the two. There do exist, however, some qualitative differences between J_{22} and J_{21} , particularly in the evolution of the surface energy near the time of initial crack growth (shown in Figure 7 (c)). The exact solution, clearly, has a zero surface energy before the initial crack starts to propagate. However, the computations with the generalised Ambrosio–Tortorelli functionals allow an uncracked body with nonzero surface energy. This occurs when the phase-field variable takes values between zero and one at the crack tip, so that the body can be classified neither as cracked nor as uncracked, but in transition. Figure 7 (c) shows that J_{22} has a relatively long transition period in comparison to J_{21} , whose surface energy evolves in a manner much closer to the exact solution in this region.

Figure 8 shows the final v -field computed by the functionals J_{22} , J_{21} , J_{12} and J_{11} . The profiles exhibit similar properties to those seen in the one-dimensional example. In particular, the phase-field variables computed by J_{21} and J_{11} have a compactly supported transition region, outside of which $v \equiv 1$. Similarly, the phase-field variables computed by J_{12} and J_{11} have a compactly supported cracked region in which $v \equiv 0$. Note, however, that this cracked region (computed by J_{12} and J_{11}) is larger than the associated region computed by J_{22} and J_{21} , particularly near $y = 0$. This is the reason for the over-estimated surface energy in Figure 7.

We now examine the performance of the Adaptive Algorithm for J_{22} , J_{21} , J_{12} and J_{11} . Figure 9 shows the mesh generated by the adaptive algorithm for the functionals at the time of failure. The number of elements in each mesh is 497233, 239489, 376030 and 218468, respectively. The smallest elements in each mesh have diameters of order 10^{-6} , 10^{-5} , 10^{-7} and 10^{-7} , respectively. The total number of linear systems solved by Adaptive Algorithm was 3050, 3135, 4167 and 2848 for each functional, respectively.

In conclusion, for the example presented in this section J_{21} produced the best results out of the four functionals considered, computing the most accurate energies with relatively few elements. The results produced using the standard Ambrosio–Tortorelli functional J_{22} were similar to those of J_{21} . In contrast, the energies computed with the functionals J_{12} and J_{11} were highly inaccurate; hence, if we wish to exploit the benefits of using these functionals — namely, the desirable properties possessed by the theoretical profiles of the resulting phase-field and displacement variables seen in Figure 6 — a better solver must be developed.

7. CONCLUSION

We have presented an adaptive algorithm for computing numerical local minimizers of the generalised Ambrosio–Tortorelli functional with a bound constraint on the phase-field variable. We have shown that, provided the associated residuals tend to zero, the algorithm generates a sequence of numerical solutions that converge to a critical point of J as the termination tolerances are driven to zero.

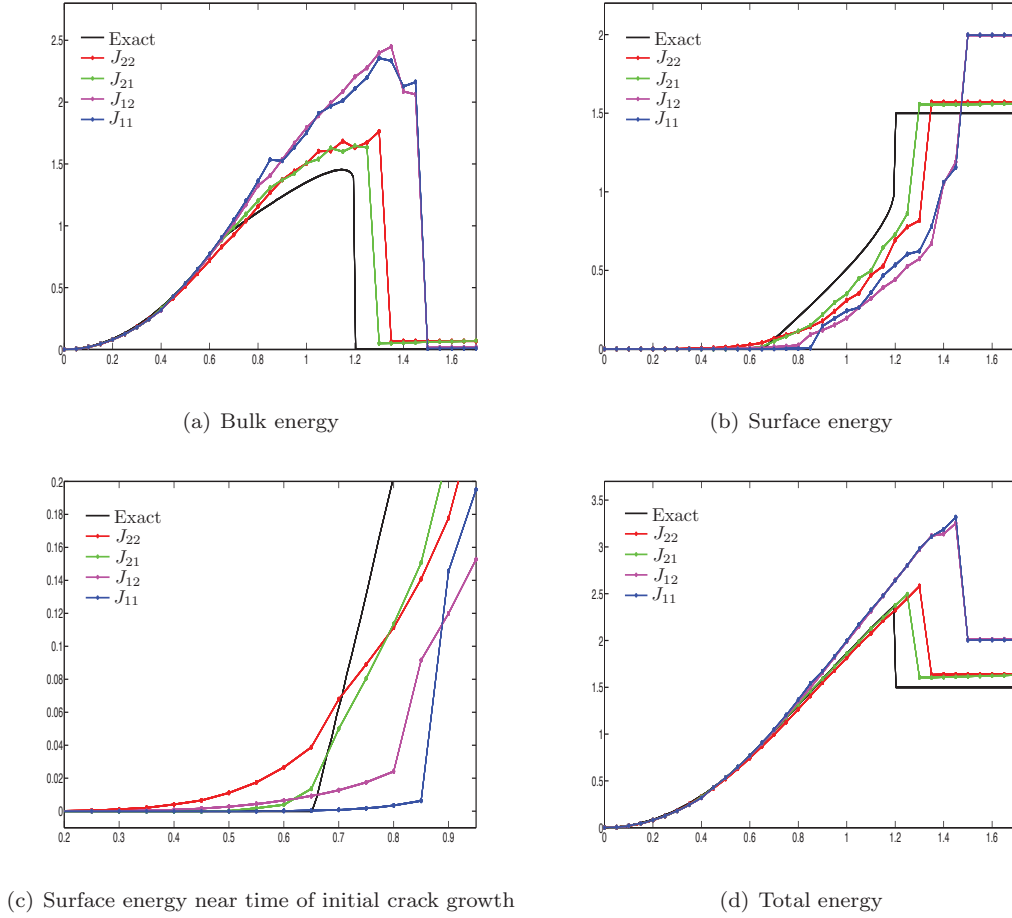
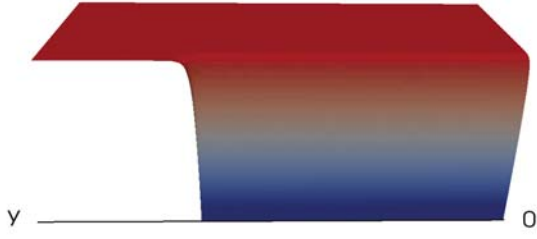
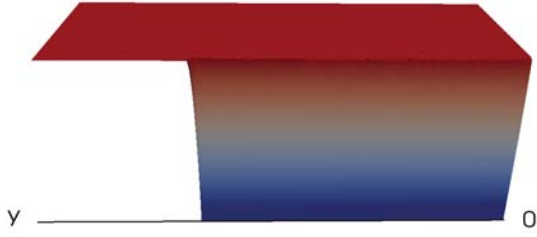
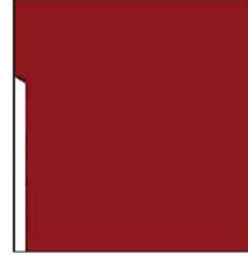
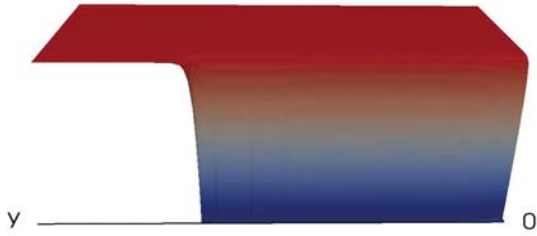
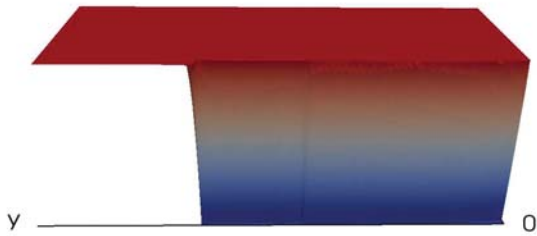


FIGURE 7. A comparison of the bulk, surface and total energies computed using the generalised Ambrosio–Tortorelli functionals J_{22} , J_{21} , J_{12} and J_{11} .

We have implemented the algorithm for a two-dimensional anti-plane strain example, which examined the effect of using a monotonicity condition to implement the irreversibility of the crack and the effect of using three alternative generalised functionals (to the standard choice). We conclude that the proposed monotonicity condition on the phase-field variable is a feasible method for implementing crack irreversibility, provided the tolerance $MCTOL$ is suitably chosen. We also conclude that the generalised functional J_{21} is a viable alternative to the standard Ambrosio–Tortorelli functional. In fact, there is a basis for it being the preferred option — producing a compactly supported cracked region and computing more accurate energies with fewer elements. Unfortunately, the algorithm performed poorly using the generalised functionals J_{11} and J_{12} , computing inaccurate energies. However, the associated displacement and phase-field profiles possess certain desirable properties; thus, if the algorithm could be improved to compute minimizers with greater efficiency and accuracy one of these may well be a favourable choice.

We believe that there are a number of possible directions for further research. We first discuss improvements to the algorithm itself. A relatively simple algorithm was used for the bound-constrained minimization algorithm with respect to v and some benefit may be gained from using a more sophisticated algorithm that is better tuned to the problem at hand. It may also be useful to consider an alternative to the alternating minimization

(a) $F(v) = v^2, G = \frac{1}{4}(1-v)^2$ (b) $F(v) = v^2, G = \frac{1}{4}(1-v)^2$ (c) $F(v) = v^2, G = \frac{9}{64}(1-v)$ (d) $F(v) = v^2, G = \frac{9}{64}(1-v)$ (e) $F(v) = v, G = \frac{1}{4}(1-v)^2$ (f) $F(v) = v, G = \frac{1}{4}(1-v)^2$ (g) $F(v) = v, G = \frac{9}{64}(1-v)$ (h) $F(v) = v, G = \frac{9}{64}(1-v)$ FIGURE 8. A comparison of the final computed v -field.

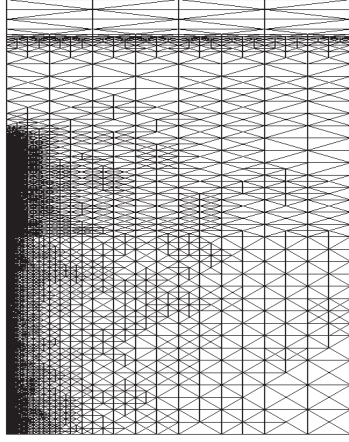
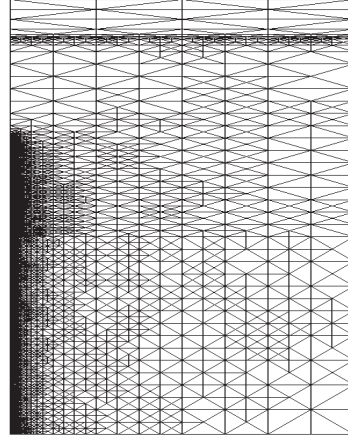
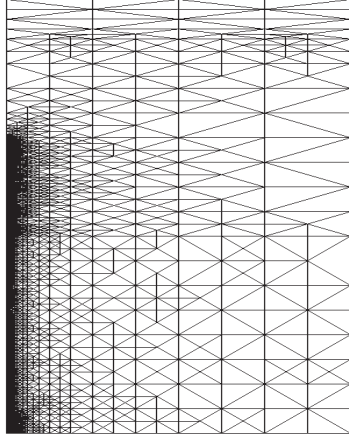
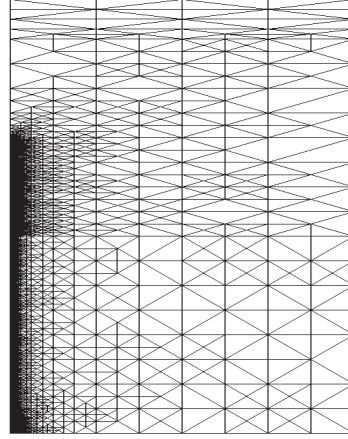
(a) $F(v) = v^2, G = \frac{1}{4}(1-v)^2$ (b) $F(v) = v^2, G = \frac{9}{64}(1-v)$ (c) $F(v) = v, G = \frac{1}{4}(1-v)^2$ (d) $F(v) = v, G = \frac{9}{64}(1-v)$

FIGURE 9. A comparison of the final mesh using the generalised Ambrosio–Tortorelli functionals J_{22} , J_{21} , J_{12} and J_{11} . The number of elements in each mesh is 497233, 239489, 376030 and 218468, respectively. The total number of linear systems solved by Adaptive Algorithm for each functional was 3050, 3135, 4167 and 2848, respectively.

algorithm, which often takes a large number of iterations to converge, perhaps by minimizing J with respect to u and v together. In addition, the speed of the algorithm could be increased through the introduction of mesh coarsening and better linear solvers. Secondly, we discuss further research relating to the choice of generalised functional. For the functional J_{21} an implementation of quadratic finite elements would increase the efficiency of the algorithm (since the transition region of the phase-field variable is quadratic in this case). For the functionals J_{11} and J_{12} it would be interesting to see if the improvements suggested to the adaptive algorithm result in more accurate computations of the energies. Finally, it would be of interest to investigate other choices of generalised functional, particularly those with concave functions F and G .

APPENDIX A. PROOF OF THE QUASI-INTERPOLATION RESULTS

In this appendix we prove Proposition 4.2 from Section 4.1.

A.1. Properties of the Mesh

We begin by reminding the reader of the definition of the mesh and proving a number of associated properties.

Recall that Ω is a polyhedral domain in \mathbb{R}^N , which contains an open subset Ω_D of positive N -dimensional Lebesgue measure. Let \mathcal{T}_h be a subdivision of Ω into N -dimensional open simplices $T \in \mathcal{T}_h$, such that $\overline{\Omega} = \cup_{T \in \mathcal{T}_h} \overline{T}$ and $T_i \cap T_j = \emptyset$ for $T_i, T_j \in \mathcal{T}_h$ with $i \neq j$. The subdivision \mathcal{T}_h is chosen in such a way that the boundary of Ω_D is discretised as the union of faces of simplices from \mathcal{T}_h .

Each simplex $T \in \mathcal{T}_h$ is taken to be an affine transformation of the open unit simplex

$$\hat{T} := \{\hat{x} = (\hat{x}_1, \dots, \hat{x}_N) : 0 < \hat{x}_i, i = 1, \dots, N, 0 < \hat{x}_1 + \dots + \hat{x}_N < 1\}. \quad (40)$$

For all $T \in \mathcal{T}_h$ we define $h_T := \text{diam}(T)$, d_T to be the diameter of the largest N -dimensional ball contained in T and $h := \max_{T \in \mathcal{T}_h} \text{diam}(T)$.

We assume that the subdivision is conforming, that is, the intersection of the closure of any two elements is either empty or is along an entire k -dimensional face, $1 \leq k \leq N - 1$. We also require that the subdivision is shape-regular, i.e.,

$$\sup_{T \in \mathcal{T}_h} \frac{h_T}{d_T} \leq \rho, \quad (41)$$

for some constant $\rho \in (0, \infty)$, which is independent of h . From now on we use the term ‘shape-regular’ to refer to a subdivision or simplex satisfying (41) with this constant.

Let \mathcal{E}_h denote the set of $(N - 1)$ -dimensional open faces in the subdivision and $E_h := \cup_{e \in \mathcal{E}_h} e$. For a face $e \in E_h$ define $h_e := \text{diam}(e)$.

Let N_h denote an index set for the vertices in the subdivision \mathcal{T}_h . For each vertex $i \in N_h$, let x_i denote the position of the i th vertex and let ζ_i be the continuous piecewise linear basis function such that $\zeta_i(x_j) = \delta_{ij}$. Define $N_h^D := \{i \in N_h : x_i \in \overline{\Omega}_D\}$ and $N_h^F := N_h \setminus N_h^D$. For each vertex $i \in N_h$, define the *patch* $\omega_i := \text{supp}(\zeta_i)$, $h_i := \text{diam}(\omega_i)$ and d_i to be the diameter of the largest N -dimensional ball contained in ω_i . Define the *shape-coefficients* $\gamma_i := \frac{1}{|\omega_i|} \int_{\omega_i} \zeta_i \, dx$.

Since the subdivision is shape-regular, it can be proved (cf. [6, 7]) that:

- P1. There exists a constant $M > 0$, independent of h , such that ω_i contains at most M elements for all $i \in N_h$.
- P2. There exists a constant $k_1 > 0$, independent of h , such that for all $i \in N_h$;

$$h_T \leq h_i \leq k_1 h_T \quad \forall T \subset \omega_i.$$

- P3. There exists a constant $k_2 > 0$, independent of h , such that for all $i \in N_h$;

$$\frac{h_i}{d_i} \leq k_2 \rho.$$

- P4. There exists a constant $k_3 > 0$, independent of h , such that for all $i, j \in N_h$ with $\mathcal{L}^N(\omega_i \cap \omega_j) > 0$;

$$h_i \leq \text{diam}(\omega_i \cup \omega_j) \leq k_3 h_i.$$

- P5. For all $e \in \mathcal{E}_h$ such that $e \subset \partial T$ for some $T \in \mathcal{T}_h$;

$$h_e \leq h_T \leq \rho h_e.$$

It will be useful in the next section to map from one element to another using the following lemma.

Lemma A.1. *Let \hat{T} and $T = \Psi(\hat{T})$ be two affine-equivalent shape-regular simplices, where*

$$\Psi(\hat{x}) = A\hat{x} + b \quad \forall \hat{x} \in \hat{T},$$

for some $A \in \mathbb{R}^{N \times N}$ and $b \in \mathbb{R}^N$, is an invertible affine mapping. Let $h_{\hat{T}}$ and h_T denote the diameter of \hat{T} and T , respectively.

Then,

$$\|A\|_2 \leq \rho \frac{h_T}{h_{\hat{T}}}, \quad \|A^{-1}\|_2 \leq \rho \frac{h_{\hat{T}}}{h_T} \quad \text{and} \quad \rho^{-N} \frac{h_T^N}{h_{\hat{T}}^N} \leq |\det(A)| \leq \rho^N \frac{h_T^N}{h_{\hat{T}}^N}.$$

Proof. Let $d_{\hat{T}}$ and d_T denote the diameter of the largest N -dimensional ball contained within \hat{T} and T , respectively. Using the result from Ciarlet [19, Section 3.1], we have

$$\|A\|_2 \leq \frac{h_T}{d_{\hat{T}}}, \quad \|A^{-1}\|_2 \leq \frac{h_{\hat{T}}}{d_T} \quad \text{and} \quad |\det(A)| = \frac{|T|}{|\hat{T}|}.$$

By shape-regularity we have $(d_{\hat{T}})^{-1} \leq \rho h_{\hat{T}}^{-1}$ and $d_T^{-1} \leq \rho h_T^{-1}$, thus

$$\|A\|_2 \leq \rho \frac{h_T}{h_{\hat{T}}}, \quad \text{and} \quad \|A^{-1}\|_2 \leq \rho \frac{h_{\hat{T}}}{h_T}.$$

Since

$$\sigma_N d_T^N \leq |T| \leq \sigma_N h_T^N \quad \text{and} \quad \sigma_N d_{\hat{T}}^N \leq |\hat{T}| \leq \sigma_N h_{\hat{T}}^N,$$

where σ_N is the measure of the N -dimensional unit ball, it follows that

$$\rho^{-N} \frac{h_T^N}{h_{\hat{T}}^N} \leq \frac{d_T^N}{h_{\hat{T}}^N} \leq |\det(A)| \leq \frac{h_T^N}{d_{\hat{T}}^N} \leq \rho^N \frac{h_T^N}{h_{\hat{T}}^N}.$$

□

Remark A.2. For all $i \in N_h$, it is possible to obtain upper and lower bounds on the shape-regularity coefficient γ_i , independently of the patch ω_i . To see this consider a patch of elements ω_i and let \hat{T} be the open unit simplex given by (40). For each $T \subset \omega_i$, let $\Psi_T : \hat{T} \mapsto T$ be such that

$$\Psi_T(\hat{z}) = A_T \hat{z} + b_T \quad \forall \hat{z} \in \hat{T},$$

for some $A_T \in \mathbb{R}^{N \times N}$ and $b_T \in \mathbb{R}^N$. For all $x \in T$, define $\hat{x} := \Psi_T^{-1}(x)$ and $\hat{\zeta}_i := \zeta_i \circ \Psi_T$.

Then,

$$\gamma_i = \frac{1}{|\omega_i|} \sum_{T \subseteq \omega_i} \int_T \zeta_i \, dx = \frac{1}{|\omega_i|} \sum_{T \subseteq \omega_i} |\det A_T| \int_{\hat{T}} \hat{\zeta}_i \, d\hat{x}.$$

Thus, using Lemma A.1 with $h_{\hat{T}} = 1$; property P2; and property P3, we have

$$\gamma_i \leq \frac{1}{\sigma_N d_i^N} \sum_{T \subseteq \omega_i} \rho^N h_T^N \frac{1}{N!} \leq \sigma_N^{-1} k_2^N \rho^{2N} \frac{M}{N!}, \quad (42)$$

$$\gamma_i \geq \frac{1}{|\omega_i|} \sum_{T \subseteq \omega_i} \rho^{-N} h_T^N \frac{1}{N!} \geq \frac{1}{\sigma_N h_i^N} \rho^{-N} \frac{h_i^N}{k_1^N} \frac{1}{N!} = (\sigma_N \rho^N k_1^N N!)^{-1}. \quad (43)$$

We can similarly obtain an upper bound on $\|\nabla \zeta_i\|_{L^\infty(T)}$, for $T \subseteq \omega_i$, in terms of h_i . Let $\nabla = (\frac{\partial}{\partial x_1}, \dots, \frac{\partial}{\partial x_N})^T$ and $\hat{\nabla} = (\frac{\partial}{\partial \hat{x}_1}, \dots, \frac{\partial}{\partial \hat{x}_N})^T$.

For all $T \subseteq \omega_i$,

$$|\nabla \zeta_i| = |A_T^{-1} \hat{\nabla} \zeta_i| \leq \|A_T^{-1}\|_2 |(-1, \dots, -1)| \leq \frac{\rho}{h_T} \sqrt{N} \leq \frac{k_1 \rho}{h_i} \sqrt{N},$$

hence,

$$h_i \|\nabla \zeta_i\|_{L^\infty(T)} \leq k_1 \rho \sqrt{N}. \quad (44)$$

A.2. Approximation and Stability Results

In this section we prove Propositions 4.2 from Section 4.1. The results are shown for the quasi-interpolation operator $\mathcal{I}_h^D : H_D^1(\Omega) \rightarrow X_h^D$; however, it is easily seen from the proofs that the results also hold for the quasi-interpolation operator $\mathcal{I}_h : H^1(\Omega) \rightarrow X_h$, by taking $N_h^F = N_h$.

We first remind the reader of the definition of the quasi-interpolation operator $\mathcal{I}_h^D : H_D^1(\Omega) \rightarrow X_h^D$. Recall that, for all $i \in N_h^F$,

$$\bar{\zeta}_i(x) := \frac{\zeta_i(x)}{\zeta(x)}, \quad \text{where} \quad \zeta(x) := \sum_{i \in N_h^F} \zeta_i(x).$$

For $f \in H_D^1(\Omega)$, the quasi-interpolant is defined as follows:

$$\mathcal{I}_h^D f := \sum_{i \in N_h^F} f_i \zeta_i(x), \quad \text{where} \quad f_i := \frac{\int_{\omega_i} f \bar{\zeta}_i \, dx}{\int_{\omega_i} \zeta_i \, dx}.$$

We now prove the following approximation result stated in Proposition 4.2 (a).

Proposition A.3. *There exists a constant $\hat{C}_1 > 0$, independent of ω_i , such that,*

$$\|(f - f_i \zeta) \bar{\zeta}_i\|_{L^2(\omega_i)} \leq \hat{C}_1 h_i \|\nabla f\|_{L^2(\bar{\omega}_i)} \quad \forall f \in H_D^1(\Omega) \text{ and } \forall i \in N_h^F,$$

where $\bar{\omega}_i$ is a patch of elements, defined by (47) and (48) in the proof, such that $\omega_i \subseteq \bar{\omega}_i$.

Proof. The structure of the proof is dependent on the location of ω_i relative to the boundary. There are two cases to consider: firstly, when $i \in N_1 := \{i \in N_h^F : \zeta_i \equiv \bar{\zeta}_i \text{ on } \omega_i\}$; and secondly, when $i \in N_2 := \{i \in N_h^F : \zeta_i \not\equiv \bar{\zeta}_i \text{ on } \omega_i\}$. In the first case we can make use of an existing interpolation result by Verfürth [34]. However, in the second case the argument is slightly more involved and we first map each patch to one of finitely many reference patches and then prove the result on the reference domain.

Case 1: We first consider patches ω_i with $i \in N_1$, on which $\zeta \equiv 1$ and $\bar{\zeta}_i \equiv \zeta_i$, hence

$$\|(f - f_i \zeta) \bar{\zeta}_i\|_{L^2(\omega_i)}^2 = \|(f - f_i) \zeta_i\|_{L^2(\omega_i)}^2 \leq \|(f - f_i) \zeta_i^{1/2}\|_{L^2(\omega_i)}^2.$$

It follows from the local averaging property (20) that for any constant $\alpha \in \mathbb{R}$, we have

$$\begin{aligned}
\|(f - f_i)\zeta_i^{1/2}\|_{L^2(\omega_i)}^2 &\leq \|(f - f_i)\zeta_i^{1/2}\|_{L^2(\omega_i)}^2 + \|\alpha\zeta_i^{1/2}\|_{L^2(\omega_i)}^2 \\
&= \int_{\omega_i} |f - f_i|^2 \zeta_i \, dx + \alpha^2 \int_{\omega_i} \zeta_i \, dx - 2\alpha \int_{\omega_i} (f - f_i)\zeta_i \, dx \\
&= \|(f - f_i - \alpha)\zeta_i^{1/2}\|_{L^2(\omega_i)}^2 \\
&\leq \|f - f_i - \alpha\|_{L^2(\omega_i)}^2.
\end{aligned} \tag{45}$$

We now simply choose

$$\alpha = (f)_{\omega_i} - f_i, \quad \text{where} \quad (f)_{\omega_i} := \frac{1}{|\omega_i|} \int_{\omega_i} f \, dx,$$

so that

$$\|(f - f_i)\zeta_i\|_{L^2(\omega_i)} \leq \|f - (f)_{\omega_i}\|_{L^2(\omega_i)}.$$

Thus, using the following approximation result by Verfürth [34]:

$$\|f - (f)_{\omega_i}\|_{L^2(\omega_i)} \leq \hat{C}_{N_1} h_i \|\nabla f\|_{L^2(\omega_i)}, \tag{46}$$

where \hat{C}_{N_1} is a positive constant independent of the patch ω_i , we have

$$\|(f - f_i)\zeta_i\|_{L^2(\omega_i)} \leq \hat{C}_{N_1} h_i \|\nabla f\|_{L^2(\omega_i)},$$

and for all $i \in N_1$, we define

$$\bar{\omega}_i := \omega_i. \tag{47}$$

Case 2: We now consider patches ω_i with $i \in N_2$. Note that for all $i \in N_2$ there exists $j \in N_h^D$ such that $\zeta_j \not\equiv 0$ on ω_i and $\zeta_j > 0$ on some part of Ω_D with positive surface measure. For such i and j define an extended patch

$$\bar{\omega}_i := \omega_i \cup \omega_j. \tag{48}$$

It is useful to consider certain equivalence classes $\mathcal{P}_1, \dots, \mathcal{P}_{\bar{M}}$ of extended patches, where each equivalence class contains all extended patches that have isomorphic triangulations; that is, the graphs of their connected vertices are isomorphic. Thus, two extended patches $\bar{\omega}_1$ and $\bar{\omega}_2$, with respective vertex sets $N_{\bar{\omega}_1}$ and $N_{\bar{\omega}_2}$, are equivalent if there exists a bijective map $\Lambda : N_{\bar{\omega}_1} \mapsto N_{\bar{\omega}_2}$, such that, any two vertices $i, j \in N_{\bar{\omega}_1}$ are adjacent if and only if $\Lambda(i)$ and $\Lambda(j)$ are adjacent. Here adjacency means connected by a line in the triangulation. It follows from property P1 that there exist finitely many such equivalence classes, independently of h . Note that any two extended patches in the same equivalence class have the same number of elements; the converse is, of course, not true.

We first prove the result for the equivalence class $\mathcal{P}_j = \{\bar{\omega}_{j_1}, \dots, \bar{\omega}_{j_n}\}$ (now dropping the subscript j to simplify notation). Suppose each extended patch in \mathcal{P} contains m elements, and for $i = 1, \dots, n$, let $\bar{\omega}_i = \cup_{k=1}^m \bar{T}_i^k$ and $\bar{h}_i := \text{diam}(\bar{\omega}_i)$.

We define a *reference patch* $\hat{\omega}$ for \mathcal{P} with diameter 1 as follows:

$$\hat{\omega} := \left\{ \frac{x - x_1}{\bar{h}_1} : x \in \bar{\omega}_1 \right\},$$

and also define

$$\hat{T}^k := \left\{ \frac{x - x_1}{\bar{h}_1} : x \in T_1^k \right\}, \quad k = 1, \dots, m.$$

Note that the diameter of \hat{T}^k , denoted by $h_{\hat{T}^k}$, satisfies

$$h_{\hat{T}^k} \leq \text{diam}(\hat{\omega}) = 1. \quad (49)$$

It can also be seen, using property P2, that

$$h_{\hat{T}^k} \geq \frac{1}{k_1} \text{diam}(\hat{\omega}) = \frac{1}{k_1}. \quad (50)$$

For each $\bar{\omega}_i \in \mathcal{P}$ there exists a continuous and invertible map Φ_i , which is affine on each element in the reference patch, such that $\bar{\omega}_i = \Phi_i(\hat{\omega})$ and $T_i^k = \Phi_i(\hat{T}^k)$, for $k = 1, \dots, m$. We can write

$$\Phi_i(\hat{x}) = A_i^k \hat{x} + b_i^k \quad \forall \hat{x} \in \hat{T}^k,$$

for some $A_i^k \in \mathbb{R}^{N \times N}$ and $b_i^k \in \mathbb{R}^N$, $k = 1, \dots, m$.

We are now in a position to prove the result. We have

$$\begin{aligned} \|(f - f_i \zeta) \bar{\zeta}_i\|_{L^2(\omega_i)}^2 &= \int_{\omega_i} |f - f_i \zeta|^2 |\bar{\zeta}_i|^2 dx \\ &\leq 2 \int_{\omega_i} (|f|^2 + |f_i \zeta|^2) |\bar{\zeta}_i|^2 dx \\ &\leq 2 \left(\int_{\omega_i} |f|^2 dx + \int_{\omega_i} |f_i|^2 \zeta_i dx \right). \end{aligned}$$

Let (\cdot, \cdot) denote the standard L^2 inner product, then

$$\int_{\omega_i} |f_i|^2 \zeta_i dx = \frac{|(f, \bar{\zeta}_i)|^2}{|(1, \zeta_i)|^2} \int_{\omega_i} \zeta_i dx \leq \|f\|_{L^2(\omega_i)}^2 \frac{\|\bar{\zeta}_i\|_{L^2(\omega_i)}^2}{|(1, \zeta_i)|} \leq \|f\|_{L^2(\omega_i)}^2 \frac{|\omega_i|}{|(1, \zeta_i)|} = \gamma_i^{-1} \|f\|_{L^2(\omega_i)}^2.$$

Therefore,

$$\|(f - f_i \zeta) \bar{\zeta}_i\|_{L^2(\omega_i)}^2 \leq 2(1 + \gamma_i^{-1}) \|f\|_{L^2(\omega_i)}^2 \leq 2(1 + \gamma_i^{-1}) \|f\|_{L^2(\bar{\omega}_i)}^2.$$

We now map $\bar{\omega}_i$ to the reference patch $\hat{\omega}$, letting $\hat{x} := \Phi_i^{-1}(x)$ and $\hat{f} := f \circ \Phi_i$. Then, by Lemma A.1, we have

$$\|f\|_{L^2(\bar{\omega}_i)}^2 = \sum_{k=1}^m \int_{T_i^k} |f|^2 dx = \sum_{k=1}^m |\det(A_i^k)| \int_{\hat{T}^k} |\hat{f}|^2 d\hat{x} \leq \sum_{k=1}^m \rho^N \frac{h_{T_i^k}^N}{h_{\hat{T}^k}^N} \|\hat{f}\|_{L^2(\hat{T}^k)}^2.$$

Thus, using (50) and property P4

$$\|f\|_{L^2(\bar{\omega}_i)}^2 \leq \rho^N k_1^N \bar{h}_i^N \|\hat{f}\|_{L^2(\hat{\omega})}^2 \leq \rho^N k_1^N k_3^N h_i^N \|\hat{f}\|_{L^2(\hat{\omega})}^2.$$

Note that $\hat{\omega}$ is an connected open domain with $\hat{f} = 0$ on a subset of $\partial \hat{\omega}$ with positive surface measure. Therefore, by a variant of Friedrichs' inequality [11, Chapter 2, Section 1.5], there exists a constant $c_2 > 0$ such

that

$$\|\hat{f}\|_{L^2(\hat{\omega})}^2 \leq c_2 \|\hat{\nabla} \hat{f}\|_{L^2(\hat{\omega})}^2.$$

We now map back to the original patch, noting that by Lemma A.1, (49) and (50) we have

$$\begin{aligned} & \|\hat{\nabla} \hat{f}\|_{L^2(\hat{\omega})}^2 \\ &= \sum_{k=1}^m \int_{\hat{T}^k} |\hat{\nabla} \hat{f}|^2 d\hat{x} = \sum_{k=1}^m \frac{1}{|\det(A_i^k)|} \int_{T_i^k} |A_i^k \nabla f|^2 dx \leq \sum_{k=1}^m \frac{\rho^N}{h_{T_i^k}^N} \rho^2 k_1^2 h_{T_i^k}^2 \|\nabla f\|_{L^2(T_i^k)}^2. \end{aligned}$$

Hence, using properties P2 and P4

$$\|\hat{\nabla} \hat{f}\|_{L^2(\hat{\omega})}^2 \leq \sum_{k=1}^m \frac{\rho^N k_1^N}{\bar{h}_i^N} \rho^2 k_1^2 \bar{h}_i^2 \|\nabla f\|_{L^2(T_i^k)}^2 \leq \rho^{N+2} k_1^{N+2} k_3^2 h_i^{-N+2} \|\nabla f\|_{L^2(\bar{\omega}_i)}^2.$$

Therefore,

$$\|f\|_{L^2(\bar{\omega}_i)}^2 \leq c_2 \rho^N k_1^N k_3^N h_i^N \|\hat{\nabla} \hat{f}\|_{L^2(\hat{\omega})}^2 \leq c_2 \rho^{2N+2} k_1^{2N+2} k_3^{N+2} h_i^2 \|\nabla f\|_{L^2(\bar{\omega}_i)}^2, \quad (51)$$

and

$$\|(f - f_i \zeta) \bar{\zeta}_i\|_{L^2(\omega_i)}^2 \leq 2(1 + \gamma_i^{-1}) c_2 \rho^{2N+2} k_1^{2N+2} k_3^{N+2} h_i^2 \|\nabla f\|_{L^2(\bar{\omega}_i)}^2. \quad (52)$$

Thus we have proved the result for all patches in \mathcal{P} . Define C_{N_2} to be the maximum constant appearing in (52) over all equivalence classes. The result now follows by taking

$$\hat{C}_1 := \max\{C_{N_1}, C_{N_2}\}.$$

□

Remark A.4. The extended patches, $\bar{\omega}_i$, $i \in N_h$, satisfy the following *uniform finite overlap* property: There exists a constant $\hat{C}_5 > 0$, independent of h , such that each element $T \in \mathcal{T}_h$ is a subset of at most \hat{C}_5 patches $\bar{\omega}_i$, $i \in N_h$.

To see this, note that for any $T \in \mathcal{T}_h$ the maximum number of extended patches to which T belongs is

$$\sum_{\substack{i \in N_h \\ x_i \in \bar{T}}} \#\{j \in N_h, j \neq i : x_j \in \bar{\omega}_i\}.$$

It follows from property P1 that this can be bounded as follows:

$$\sum_{\substack{i \in N_h \\ x_i \in \bar{T}}} \#\{j \in N_h, j \neq i : x_j \in \bar{\omega}_i\} \leq \sum_{\substack{i \in N_h \\ x_i \in \bar{T}}} (M+1) = N(M+1).$$

We therefore take $\hat{C}_5 = N(M+1)$, which is independent of h .

The following corollary will be needed for the proof of Proposition A.7.

Corollary A.5. *There exists a constant $\hat{C}_6 > 0$, independent of ω_i , such that*

$$\|(f - f_i) \zeta_i^{1/2}\|_{L^2(\omega_i)} \leq \hat{C}_6 h_i \|\nabla f\|_{L^2(\bar{\omega}_i)} \quad \forall f \in H_D^1(\Omega) \text{ and } \forall i \in N_h.$$

Proof. Let $f \in H_D^1(\Omega)$; then it follows from (45) and (46) that for all $i \in N_1$:

$$\|(f - f_i)\zeta_i^{1/2}\|_{L^2(\omega_i)} \leq \hat{C}_{N_1} h_i \|\nabla f\|_{L^2(\bar{\omega}_i)},$$

where \hat{C}_{N_1} is independent of ω_i .

For $i \in N_2$, we have

$$\|(f - f_i)\zeta_i^{1/2}\|_{L^2(\omega_i)}^2 \leq \|f - f_i\|_{L^2(\omega_i)}^2 \leq 2(\|f\|_{L^2(\omega_i)}^2 + \|f_i\|_{L^2(\omega_i)}^2).$$

Since

$$\|f_i\|_{L^2(\omega_i)}^2 = \frac{|(f, \bar{\zeta}_i)|^2}{|(1, \bar{\zeta}_i)|^2} |\omega_i| \leq \|f\|_{L^2(\omega_i)}^2 \frac{|\omega_i|^2}{|(1, \bar{\zeta}_i)|^2} = \gamma_i^{-2} \|f\|_{L^2(\omega_i)}^2,$$

it follows from (51) that there exists a constant $c_3 > 0$, independent of $i \in N_2$, such that

$$\|(f - f_i)\zeta_i^{1/2}\|_{L^2(\omega_i)} \leq c_3 h_i \|\nabla f\|_{L^2(\bar{\omega}_i)}.$$

Finally, for all $i \in N_h^D$, we have

$$\|(f - f_i)\zeta_i\|_{L^2(\omega_i)}^2 \leq \|f\|_{L^2(\omega_i)}^2.$$

Since $i \in N_h^D$, $\partial\omega_i \cap \Omega_D$ has positive surface measure. Hence, using a similar mapping argument to that given in the proof of Case 2 in Proposition A.3, it is easily shown that there exists a constant $c_4 > 0$, independent of $i \in N_h^D$, such that

$$\|f\|_{L^2(\omega_i)} \leq c_4 h_i \|\nabla f\|_{L^2(\omega_i)} \quad \forall i \in N_h^D.$$

For $i \in N_h^D$ we define $\bar{\omega}_i := \omega_i$. The result now follows taking $\hat{C}_6 := \max\{\hat{C}_{N_1}, c_3, c_4\}$. \square

We now prove the following stability result from Proposition 4.2 (c).

Corollary A.6. *There exist constants $\hat{C}_3 > 0$ and $\hat{C}_4 > 0$, independent of T , such that*

$$\|\mathcal{I}_h^D f\|_{L^2(T)} \leq \hat{C}_3 \|f\|_{L^2(\omega_T)} \quad \text{and} \quad \|\nabla(\mathcal{I}_h^D f)\|_{L^2(T)} \leq \hat{C}_4 \|\nabla f\|_{L^2(\bar{\omega}_T)},$$

for all $f \in H_D^1(\Omega)$ and all $T \in \mathcal{T}_h$, where $\omega_T := \bigcup_{i: x_i \in \bar{T}} \omega_i$ and $\bar{\omega}_T := \bigcup_{i: x_i \in \bar{T}} \bar{\omega}_i$.

Proof. Let $f \in H_D^1(\Omega)$ and $T \in \mathcal{T}_h$; then

$$\|\mathcal{I}_h^D f\|_{L^2(T)}^2 = \int_T \left| \sum_{\substack{i \in N_h^F \\ x_i \in \bar{T}}} f_i \zeta_i \right|^2 dx \leq (N+1) \sum_{\substack{i \in N_h^F \\ x_i \in \bar{T}}} \int_T |f_i|^2 |\zeta_i|^2 dx.$$

We have

$$\|f_i\|_{L^2(T)}^2 \leq \|f\|_{L^2(\omega_i)}^2 \frac{\|\zeta_i\|_{L^2(\omega_i)}^2}{|(1, \zeta_i)|^2},$$

and therefore

$$\|\mathcal{I}_h^D f\|_{L^2(T)}^2 \leq (N+1) \sum_{\substack{i \in N_h^F \\ x_i \in \bar{T}}} \|f\|_{L^2(\omega_i)}^2 \frac{\|\zeta_i\|_{L^2(\omega_i)}^4}{|(1, \zeta_i)|^2} \leq (N+1) \sum_{\substack{i \in N_h^F \\ x_i \in \bar{T}}} \gamma_i^{-2} \|f\|_{L^2(\omega_i)}^2.$$

Hence, using (42), we have

$$\begin{aligned}\|\mathcal{I}_h^D f\|_{L^2(T)}^2 &\leq (N+1)\sigma_N^2\rho^{2N}k_1^{2N}(N!)^2 \sum_{\substack{i \in N_h^F \\ x_i \in \bar{T}}} \|f\|_{L^2(\omega_i)}^2 \\ &\leq (N+1)^2\sigma_N^2\rho^{2N}k_1^{2N}(N!)^2 \|f\|_{L^2(\omega_T)}^2,\end{aligned}$$

and the result follows.

Now let us consider the second stability result. Since $\sum_{i:x_i \in \bar{T}} \zeta_i \equiv 1$ on T , we have, $\sum_{i:x_i \in \bar{T}} \nabla \zeta_i \equiv 0$ on T . Hence, for any $\alpha \in \mathbb{R}$

$$\begin{aligned}\|\nabla(\mathcal{I}_h^D f)\|_{L^2(T)}^2 &= \int_T \left| \sum_{i:x_i \in \bar{T}} (f_i \nabla \zeta_i - (f - \alpha) \nabla \zeta_i) \right|^2 dx \\ &\leq (N+1) \sum_{i:x_i \in \bar{T}} \int_T |f - f_i - \alpha|^2 |\nabla \zeta_i|^2 dx \\ &\leq (N+1) \sum_{i:x_i \in \bar{T}} \|\nabla \zeta_i\|_{L^\infty(T)}^2 \int_{\omega_i} |f - f_i - \alpha|^2 dx.\end{aligned}$$

Following similar arguments to those set out in the proofs of Proposition A.3 and Corollary A.5 (taking $\alpha = 0$ if $i \in N_2$ or $i \in N_h^D$) it is easily seen that there exists a positive constant c_5 , independent of ω_i , such that

$$\|f - f_i - \alpha\|_{L^2(\omega_i)}^2 \leq c_5 h_i^2 \|\nabla f\|_{L^2(\bar{\omega}_i)}^2.$$

Hence, using (44)

$$\begin{aligned}\|\nabla(\mathcal{I}_h^D f)\|_{L^2(T)}^2 &\leq c_5(N+1) \sum_{i:x_i \in \bar{T}} \|\nabla \zeta_i\|_{L^\infty(T)}^2 h_i^2 \|\nabla f\|_{L^2(\bar{\omega}_i)}^2 \\ &\leq c_5(N+1)k_1^2\rho^2N \sum_{i:x_i \in \bar{T}} \|\nabla f\|_{L^2(\bar{\omega}_i)}^2 \\ &\leq c_5(N+1)^2k_1^2\rho^2N \|\nabla f\|_{L^2(\bar{\omega}_T)}^2.\end{aligned}$$

□

We conclude by proving the following approximation result from Proposition 4.2 (b).

Proposition A.7. *There exists a constant $\hat{C}_2 > 0$, independent of e , such that*

$$\|f - \mathcal{I}_h^D f\|_{L^2(e)} \leq \hat{C}_2 h_e^{1/2} \|\nabla f\|_{L^2(\bar{\omega}_e)} \quad \forall f \in H_D^1(\Omega) \text{ and } \forall e \in E_h,$$

where $\bar{\omega}_e := \bigcup_{i:x_i \in \bar{e}} \bar{\omega}_i$.

Proof. Let $f \in H_D^1(\Omega)$ and $e \in E_h$; then

$$\begin{aligned} \|f - \mathcal{I}_h^D f\|_{L^2(e)}^2 &= \int_e \left| \sum_{i: x_i \in \bar{e}} (f\zeta_i - f_i\zeta_i) \right|^2 dx \\ &\leq N \sum_{i: x_i \in \bar{e}} \int_e |(f - f_i)\zeta_i|^2 dx \\ &\leq N \sum_{i: x_i \in \bar{e}} \sum_{\substack{T \in \mathcal{T}_h \\ e \subset \partial T}} \int_{\partial T} |(f - f_i)\zeta_i|^2 dx. \end{aligned}$$

For all $w \in W^{1,1}(T)$ there exists a constant $C > 0$, independent of $T \in \mathcal{T}_h$, such that

$$\|w\|_{L^1(\partial T)} \leq C \left[h_T^{-1} \|w\|_{L^1(T)} + \|\nabla w\|_{L^1(T)} \right].$$

This is seen by first mapping T to the unit simplex and then applying the trace theorem [23, Section 5.5 (Theorem 1)]. Thus, taking $w = (f - f_i)^2 \zeta_i^2$, it follows that

$$\begin{aligned} &\|(f - f_i)\zeta_i\|_{L^2(\partial T)}^2 \\ &\leq Ch_T^{-1} \|(f - f_i)\zeta_i\|_{L^2(T)}^2 + 2C \|(f - f_i)\zeta_i \nabla((f - f_i)\zeta_i)\|_{L^1(T)} \\ &\leq Ch_T^{-1} \|(f - f_i)\zeta_i\|_{L^2(T)}^2 + 2C \|(f - f_i)^2 \zeta_i \nabla \zeta_i\|_{L^1(T)} + 2C \|(f - f_i)\zeta_i^2 \nabla f\|_{L^1(T)} \\ &\leq Ch_T^{-1} \|(f - f_i)\zeta_i\|_{L^2(\omega_i)}^2 + 2C \|\nabla \zeta_i\|_{L^\infty(T)} \|(f - f_i)\zeta_i^{1/2}\|_{L^2(\omega_i)}^2 \\ &\quad + 2C \|(f - f_i)\zeta_i\|_{L^2(\omega_i)} \|\nabla f\|_{L^2(\omega_i)}. \end{aligned}$$

Using property P2 and (44)

$$\begin{aligned} \|(f - f_i)\zeta_i\|_{L^2(\partial T)}^2 &\leq C(k_1 + 2\rho k_1 \sqrt{N}) h_i^{-1} \|(f - f_i)\zeta_i^{1/2}\|_{L^2(\omega_i)}^2 \\ &\quad + 2C \|(f - f_i)\zeta_i^{1/2}\|_{L^2(\omega_i)} \|\nabla f\|_{L^2(\omega_i)}, \end{aligned}$$

and by Corollary A.5, we have

$$\|(f - f_i)\zeta_i^{1/2}\|_{L^2(\partial T)}^2 \leq C(k_1 + 2\rho k_1 \sqrt{N}) \hat{C}_6^2 h_i \|\nabla f\|_{L^2(\bar{\omega}_i)}^2 + 2C \hat{C}_6 h_i \|\nabla f\|_{L^2(\bar{\omega}_i)}^2.$$

Hence,

$$\|f - \mathcal{I}_h^D f\|_{L^2(e)}^2 \leq 2NC \hat{C}_6 (k_1 \hat{C}_6 + 2\rho k_1 \sqrt{N} \hat{C}_6 + 2) \sum_{i: x_i \in \bar{e}} h_i \|\nabla f\|_{L^2(\bar{\omega}_i)}^2.$$

It follows from properties P2 and P5 that $h_i \leq k_1 \rho h_e$, and therefore

$$\|f - \mathcal{I}_h^D f\|_{L^2(e)}^2 \leq N^2 C \hat{C}_6 k_1 \rho (k_1 \hat{C}_6 + 2\rho k_1 \sqrt{N} \hat{C}_6 + 2) h_e \|\nabla f\|_{L^2(\bar{\omega}_e)}^2.$$

□

REFERENCES

- [1] G. ALLAIRE, F. JOUVE, AND N. VAN GOETHEM, *A level set method for the numerical simulation of damage evolution*, in ICIAM 07—6th International Congress on Industrial and Applied Mathematics, Eur. Math. Soc., Zürich, 2009, pp. 3–22.

- [2] L. AMBROSIO, A. COSCIA, AND G. DAL MASO, *Fine properties of functions with bounded deformation*, Arch. Rational Mech. Anal., 139 (1997), pp. 201–238.
- [3] L. AMBROSIO, N. FUSCO, AND D. PALLARA, *Functions of bounded variation and free discontinuity problems*, Oxford Mathematical Monographs, The Clarendon Press Oxford University Press, New York, 2000.
- [4] H. AMORA, J.-J. MARIGO, AND C. MAURIN, *Regularized formulation of the variational brittle fracture with unilateral contact: Numerical experiments*, J. Mech. Phys. Solids, 57 (2009), pp. 1209–1229.
- [5] V. BARBU AND T. PRECUPANU, *Convexity and optimization in Banach spaces*, vol. 10 of Mathematics and its Applications (East European Series), D. Reidel Publishing Co., Dordrecht, Romanian ed., 1986.
- [6] C. BERNARDI, *Optimal finite-element interpolation on curved domains*, SIAM J. Numer. Anal., 26 (1989), pp. 1212–1240.
- [7] C. BERNARDI AND V. GIRAULT, *A local regularization operator for triangular and quadrilateral finite elements*, SIAM J. Numer. Anal., 35 (1998), pp. 1893–1916 (electronic).
- [8] B. BOURDIN, *Numerical implementation of the variational formulation for quasi-static brittle fracture*, Interfaces Free Bound., 9 (2007), pp. 411–430.
- [9] B. BOURDIN, *The variational formulation of brittle fracture: numerical implementation and extensions*, IUTAM Symposium on Discretization Methods for Evolving Discontinuities, (2007), pp. 381 – 393.
- [10] B. BOURDIN, G. A. FRANCFORT, AND J.-J. MARIGO, *Numerical experiments in revisited brittle fracture*, J. Mech. Phys. Solids, 48 (2000), pp. 797–826.
- [11] D. BRAESS, *Finite elements*, Cambridge University Press, Cambridge, third ed., 2007. Theory, fast solvers, and applications in elasticity theory, Translated from the German by Larry L. Schumaker.
- [12] A. BRAIDES, *Approximation of free-discontinuity problems*, vol. 1694 of Lecture Notes in Mathematics, Springer-Verlag, Berlin, 1998.
- [13] ———, *Γ -convergence for beginners*, vol. 22 of Oxford Lecture Series in Mathematics and its Applications, Oxford University Press, Oxford, 2002.
- [14] S. C. BRENNER AND L. R. SCOTT, *The mathematical theory of finite element methods*, vol. 15 of Texts in Applied Mathematics, Springer-Verlag, New York, second ed., 2002.
- [15] S. BURKE, C. ORTNER, AND E. SÜLI, *An adaptive finite element approximation of a variational model of brittle fracture*, SIAM Journal on Numerical Analysis, 48 (2010), pp. 980–1012.
- [16] C. CARSTENSEN, *Quasi-interpolation and a posteriori error analysis in finite element methods*, M2AN Math. Model. Numer. Anal., 33 (1999), pp. 1187–1202.
- [17] A. CHAMBOLLE, *A density result in two-dimensional linearized elasticity, and applications*, Arch. Ration. Mech. Anal., 167 (2003), pp. 211–233.
- [18] Z. CHEN AND R. H. NOCHETTO, *Residual type a posteriori error estimates for elliptic obstacle problems*, Numer. Math., 84 (2000), pp. 527–548.
- [19] P. G. CIARLET, *The finite element method for elliptic problems*, North-Holland Publishing Co., Amsterdam, 1978. Studies in Mathematics and its Applications, Vol. 4.
- [20] G. DAL MASO, G. A. FRANCFORT, AND R. TOADER, *Quasistatic crack growth in nonlinear elasticity*, Arch. Ration. Mech. Anal., 176 (2005), pp. 165–225.
- [21] E. DE GIORGI, M. CARRIERO, AND A. LEACI, *Existence theorem for a minimum problem with free discontinuity set*, Arch. Rational Mech. Anal., 108 (1989), pp. 195–218.
- [22] G. DEL PIERO, G. LANCIONI, AND R. MARCH, *A variational model for fracture mechanics: numerical experiments*, J. Mech. Phys. Solids, 55 (2007), pp. 2513–2537.
- [23] L. C. EVANS, *Partial differential equations*, vol. 19 of Graduate Studies in Mathematics, American Mathematical Society, Providence, RI, 1998.
- [24] M. FOCARDI, *On the variational approximation of free-discontinuity problems in the vectorial case*, Math. Models Methods Appl. Sci., 11 (2001), pp. 663–684.
- [25] G. A. FRANCFORT AND C. J. LARSEN, *Existence and convergence for quasi-static evolution in brittle fracture*, Comm. Pure Appl. Math., 56 (2003), pp. 1465–1500.
- [26] G. A. FRANCFORT AND J.-J. MARIGO, *Revisiting brittle fracture as an energy minimization problem*, J. Mech. Phys. Solids, 46 (1998), pp. 1319–1342.
- [27] A. GIACOMINI, *Ambrosio-Tortorelli approximation of quasi-static evolution of brittle fractures*, Calc. Var. Partial Differential Equations, 22 (2005), pp. 129–172.
- [28] A. A. GRIFFITH, *The phenomena of rupture and flow in solids*, Philosophical Transactions of the Royal Society of London, 221 (1921), pp. 163–198.
- [29] C. T. KELLEY, *Iterative methods for optimization*, vol. 18 of Frontiers in Applied Mathematics, Society for Industrial and Applied Mathematics (SIAM), Philadelphia, PA, 1999.
- [30] N. KIKUCHI AND J. T. ODEN, *Contact problems in elasticity: a study of variational inequalities and finite element methods*, vol. 8 of SIAM Studies in Applied Mathematics, Society for Industrial and Applied Mathematics (SIAM), Philadelphia, PA, 1988.

- [31] G. LANCIONI AND G. ROYER-CARFAGNI, *The variational approach to fracture mechanics. A practical application to the French panthéon in Paris*, J. Elasticity, 95 (2009), pp. 1–30.
- [32] M. NEGRI AND C. ORTNER, *Quasi-static crack propagation by Griffith's criterion*, Math. Models Methods Appl. Sci., 18 (2008), pp. 1895–1925.
- [33] J. NOCEDAL AND S. J. WRIGHT, *Numerical optimization*, Springer Series in Operations Research, Springer-Verlag, New York, 1999.
- [34] R. VERFÜRTH, *Error estimates for some quasi-interpolation operators*, M2AN Math. Model. Numer. Anal., 33 (1999), pp. 695–713.
- [35] A. J. WEIR, *Lebesgue integration and measure*, Cambridge University Press, London, 1973. Integration and measure, Vol. 1.